NUREG/CR-2757
EGG-2123

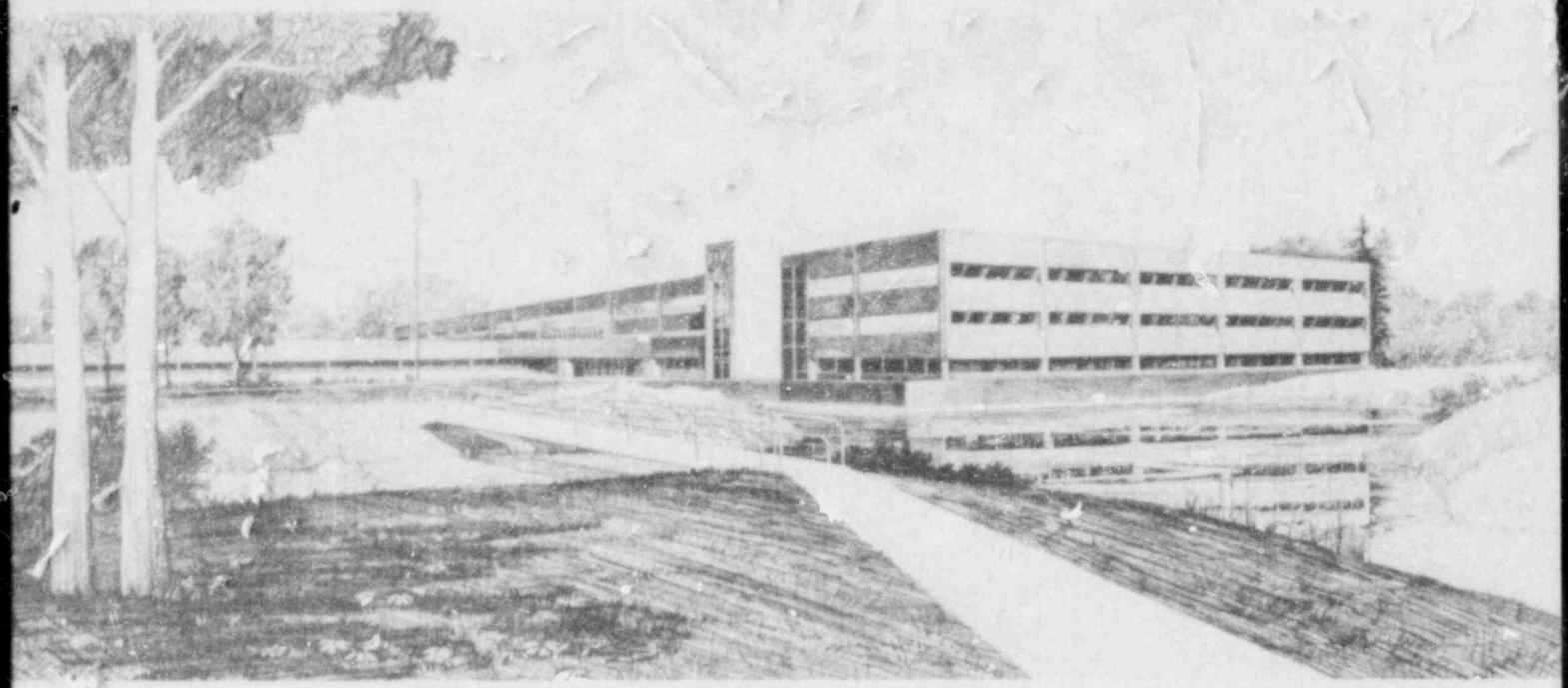

U.S. Department of Energy
Idaho Operations Office • Idaho National Engineering Laboratory

Zircaloy Cladding Embrittlement Criteria: Comparison of In-Pile and Out-of-Pile Results

Fahmy M. Haggag

July 1982

Prepared for the
U.S. Nuclear Regulatory Commission
Under DOE Contract No. DE-AC07-76IDO1570

EG&G Idaho

Available from

GPO Sales Program
Division of Technical Information and Document Control
U.S. Nuclear Regulatory Commission
Washington, D.C. 20555

and

National Technical Information Service
Springfield, Virginia 22161

NUREG/CR-2757
EGG-2123
Distribution Category: R3

ZIRCALOY CLADDING EMBRITTLEMENT CRITERIA: COMPARISON OF IN-PILE AND OUT-OF-PILE RESULTS

Fahmy M. Haggag

Published July 1982

EG&G Idaho, Inc.
Idaho Falls, Idaho 83415

Prepared for the
U.S. Nuclear Regulatory Commission
Washington, D.C. 20555
Under DOE Contract No. DE-AC07-76IDO1570
FIN No. A6041

ABSTRACT

Zircaloy-4 cladding embrittlement data from both in-pile and out-of-pile experiments are compared and correlated with embrittlement criteria based on the fraction of the remaining beta phase, the extent of oxidation (equivalent cladding reacted), and the oxygen concentration in the beta phase. The in-pile data are from the Power-Cooling-Mismatch and Irradiation Effects Test Series performed in the Power Burst Facility reactor at the Idaho National Engineering Laboratory. The out-of-pile data are from isothermal oxidation experiments conducted at Argonne National Laboratory on simulated fuel rods in high-temperature steam. The zircaloy embrittlement criteria most applicable to severe fuel damage conditions are identified.

SUMMARY

The applicability of various embrittlement criteria for zircaloy-4 cladding to severe fuel damage conditions was investigated through the use of in-pile and out-of-pile data. In-pile data were derived from the postirradiation examination of 56 light water reactor-type fuel rods under postulated accident conditions in 16 separate experiments. These experiments were performed in the Power Burst Facility (PBF) reactor at the Idaho National Engineering Laboratory as part of the Thermal Fuels Behavior Program conducted by EG&G Idaho, Inc., for the U.S. Nuclear Regulatory Commission. The out-of-pile data were obtained from embrittlement studies of simulated fuel rods that had been isothermally oxidized in high-temperature steam at the Argonne National Laboratory (ANL).

The PBF and ANL tests were investigated to evaluate the zircaloy embrittlement criteria based on fractional thickness of the remaining beta phase (F_W), equivalent cladding reacted (ECR), and oxygen content in the beta phase; and a failure boundary based on time-at-oxidation temperature.

The embrittlement criterion of $F_W \leq 0.5$ accounted for both PBF and ANL thermal shock failures, while several in-pile and out-of-pile handling failures were not predicted by that criterion. The 17% ECR criterion was consistent with the thermal shock failures from both the PBF and ANL tests, but several in-pile handling failures and one out-of-pile handling failure were not predicted by that criterion. The PBF data satisfied the Chung and Kassner criterion for thermal shock (thickness of the cladding with $\leq$0.9 wt% oxygen should be greater than 0.1 mm to survive quenching). Only three failures from two rods operated during film boiling testing with breached cladding were not predicted by the Chung and Kassner criterion for handling failure (thickness of the cladding with $\leq$0.7 wt% oxygen should be greater than 0.3 mm). Pawel's criteria of 95% oxygen saturation of beta-zircaloy and 0.7 wt% oxygen fit the in-pile thermal shock failures as well as the handling failures except for the three PBF failures that also were not predicted by Chung and Kassner's criterion for handling failure. Pawel's criteria require only knowledge of oxidation time and temperature whereas Chung and Kassner's criteria require, in addition, a sophisticated calculation of the oxygen concentration through the cladding. Therefore, Pawel's criteria are simpler to apply. However, Pawel's criteria do not distinguish the cause of rod failure (quenching or handling). For the PBF Severe Fuel Damage Tests, where it is important to distinguish whether rod failure occurred upon quenching or during subsequent handling, the embrittlement criteria of Chung and Kassner are most appropriate.

ACKNOWLEDGMENTS

Dr. S. L. Seiffert (The BDM Corporation) is acknowledged for his valuable discussions, comments, and revision of the PBF data; Dr. H. M. Chung (Argonne National Laboratory) for his fruitful discussions; and Dr. D. W. Croucher, Dr. R. R. Hobbins, and Mr. P. E. MacDonald (EG&G Idaho, Inc.) for their review of and comments on this report. The efforts of Dr. D. L. Hagrman and Mr. R. E. Mason (EG&G Idaho, Inc.) in the computational work are greatly appreciated. Finally, the author thanks G. S. Reilly and P. B. Hembree for their help with the necessary computer runs and plots for this report.

CONTENTS

FIGURES

TABLES

ZIRCALOY CLADDING EMBRITTLEMENT CRITERIA: COMPARISON OF IN-PILE AND OUT-OF-PILE RESULTS

1. INTRODUCTION

The safe operation of nuclear power reactors requires continuing investigation of the likelihood and consequences of transient events capable of achieving high fuel and cladding temperatures. During a high-temperature transient accident, steam oxidation of the zircaloy cladding can have a detrimental effect upon the rod behavior because thick reaction layers of brittle oxide and oxygen-stablized alpha zircaloy can form. Embrittled cladding can also fragment upon introduction of emergency cooling water in a severe accident. Limits specifying the amount of oxidation are required to preclude a loss of coolable geometry.

In response to the Three Mile Island (TMI) accident, the United States Nuclear Regulatory Commission recently initiated a severe core damage assessment program.[1] One phase of this program, the Severe Fuel Damage (SFD) Test Series, will be conducted in the Power Burst Facility (PBF) at the Idaho National Engineering Laboratory (INEL). In these tests, the behavior of fuel rods will be studied under prolonged conditions that cause the coolant to boil off and uncover the fuel rods. The fuel rod cladding will become extensively oxidized in a high-temperature steam environment. The introduction of cooling water at the termination of the transient might then cause rapid quenching and fragmentation of the test fuel rod bundle. Identifying the most suitable criteria for predicting cladding embrittlement is necessary to predict the posttransient physical state of the SFD test bundle and, hence, the damage state of the TMI-2 core.

An evaluation of oxygen embrittlement of zircaloy cladding and the applicability of various criteria for the embrittlement of the cladding at room temperature are the subject of this report. The data evaluated were obtained from post-irradiation examinations of 56 light water reactor (LWR)-type nuclear fuel rods tested in 16 in-pile experiments in the Power Burst Facility (PBF) reactor at the Idaho National Engineering Laboratory (INEL). These fuel behavior studies have been conducted for the Nuclear Regulatory Commission by the Thermal Fuels Behavior Program of EG&G Idaho, Inc., to provide an experimental data base for assessment of reactor safety issues and for development and assessment of computer models to calculate fuel rod behavior.[2,3] They include the Power-Cooling-Mismatch (PCM) and Irradiation Effects (IE) Test Series. Out-of-pile data[2] obtained from isothermal oxidation experiments conducted at Argonne National Laboratory (ANL) on simulated fuel rods in high-temperature steam are compared with the PBF data in this report. It also includes more complete and accurate comparison of zircaloy embrittlement between the in-pile and out-of-pile test results than that presented in a previous report by Seiffert and Hobbins.[4] The improvement of the comparison between the PBF and the ANL experiment results is mainly due to the modification of the COBILD computer code.[5]

The objectives of this report are to:

1. Compare the different embrittlement parameters (fraction of the remaining beta phase, equivalent cladding reacted, and oxygen concentration in the beta phase) obtained from both PBF in-pile and ANL out-of-pile tests.

2. Analyze and discuss the applicability of the various embrittlement criteria developed from out-of-pile experiments to the in-pile PBF test results.

3. Identify the zircaloy embrittlement criteria most suitable for predicting the PBF SFD results and the damage state of the TMI-2 core.

Section 2 contains a brief description of the in-pile test conditions, test cladding characterization, experiment configuration, and observations of the effects of film boiling operation on test rods. Analysis of the in-pile test results, and comparison of embrittlement criteria and parameters developed from out-of-pile experiments with those results are discussed in Section 3. Finally, Section 4 presents a discussion of results and conclusions derived from the comparison of the embrittlement parameters obtained from in-pile testing with those from out-of-pile tests.

2. SUMMARY OF EXPERIMENT TEST CONDITIONS AND RESULTS

The ANL out-of-pile tests[2] were conducted on zircaloy-4 cladding samples isothermally oxidized in high-temperature steam. Cladding samples 200 mm long, 10.9 mm in outer diameter, and 0.635 mm in wall thickness were filled with high-purity recrystallized alumina pellets and pressurized with helium or argon at 6.89 MPa to simulate nuclear fuel rods. These rods were direct-resistance-heated in steam. The results of these out-of-pile embrittlement studies are used for comparison with the in-pile PBF results.[4,6,7] The test conditions, cladding characterization, experiment details, and rod damage characterization for the in-pile PBF tests are discussed in the following subsections.

2.1 Test Conditions

Zircaloy embrittlement was evaluated from data derived from the postirradiation examination of 56 pressurized water reactor-type fuel rods tested in 16 separate in-pile experiments. Two categories of tests were conducted in the PBF reactor in-pile test loop: power cooling-mismatch (PCM) and irradiation effects (IE). The rods were tested in a pressurized water loop under operating conditions similar to those in a commercial pressurized water reactor. The test region, located in the center of the PBF reactor, operates as a neutron flux trap, permitting high power densities in test rods relative to the power level of the rods in the surrounding driver core.[8] The PCM tests were designed to evaluate the effects of different thermal-hydraulic conditions on the high-temperature transient behavior of previously unirradiated zircaloy-clad rods. The IE tests were performed to investigate the effects of prior irradiation history (burnup to a maximum of 16 GWd/tU) and rod design variables (fuel density, diametral gap, and internal pressure) on rod behavior during PCM conditions. Reference 9 presents an overview of the PCM and IE test series. Specific details of test design, individual test objectives, and the results for each test are given in References 10-30.

2.2. Test Cladding Characterization

Each fuel rod used in the PCM test series was composed of UO_2 pellets contained in zircaloy-4 cladding. The 0.914-m-long fuel stack contained 60 dished pellets of 93% theoretical density (20 wt% ^{235}U enriched UO_2). Each of the previously irradiated rods in the IE tests contained 56 dished UO_2 pellets (9.5 or 12.5 wt% ^{235}U enriched UO_2) in a nominal active fuel stack length of 0.88 m. Test rods assembled from unirradiated pellets and irradiated cladding tubes had nominal characteristics of a 9.95-mm-outside diameter and a 0.59- to 0.62-mm cladding wall thickness containing ~40 weight ppm hydrogen prior to the PCM testing. The cladding of the fresh rods had a pretest nominal outside diameter of 10.72 mm and a 0.59-0.62-mm wall thickness, and contained <10 weight ppm hydrogen. The crystallographic texture of the cladding indicated a slight preference for basal pole alignment along the tangential direction with a texture factor $f \simeq 0$. Postirradiation examination showed that hydrides tended to precipitate circumferentially.

2.3 Experiment Details

The rods were tested singly or in groups of four, with the exception of one nine-rod bundle test. A test rod with its instrumentation and flow shroud is shown in Figure 1. Variations within the individual shrouds of up to ±5% in the coolant mass flux and rod power occurred among the rods tested four at a time. The PCM and IE test assemblies generally were instrumented for measurement of coolant temperature and flow conditions, rod length change, rod internal pressure, fuel centerline temperature (unirradiated rods only), plenum gas temperature, cladding surface temperatures, and the instantaneous and integrated relative neutron flux profile in the region of the rods. The specific test instrumentation was selected on the basis of the individual test objectives.

The basic PBF test sequence consisted of a thermal-hydraulic power calibration, a preconditioning operation, and the film boiling testing. The preconditioning operation allowed for pellet cracking and partial restructuring of the UO_2 fuel. Film boiling, in these tests, was achieved by either decreasing the coolant flow rate or increasing the reactor power at low, steady coolant flow while maintaining the coolant pressure at 15 MPa. Peak rod powers ranged from 49 to nominally 84 kW/m. The heating rates were generally in the range of

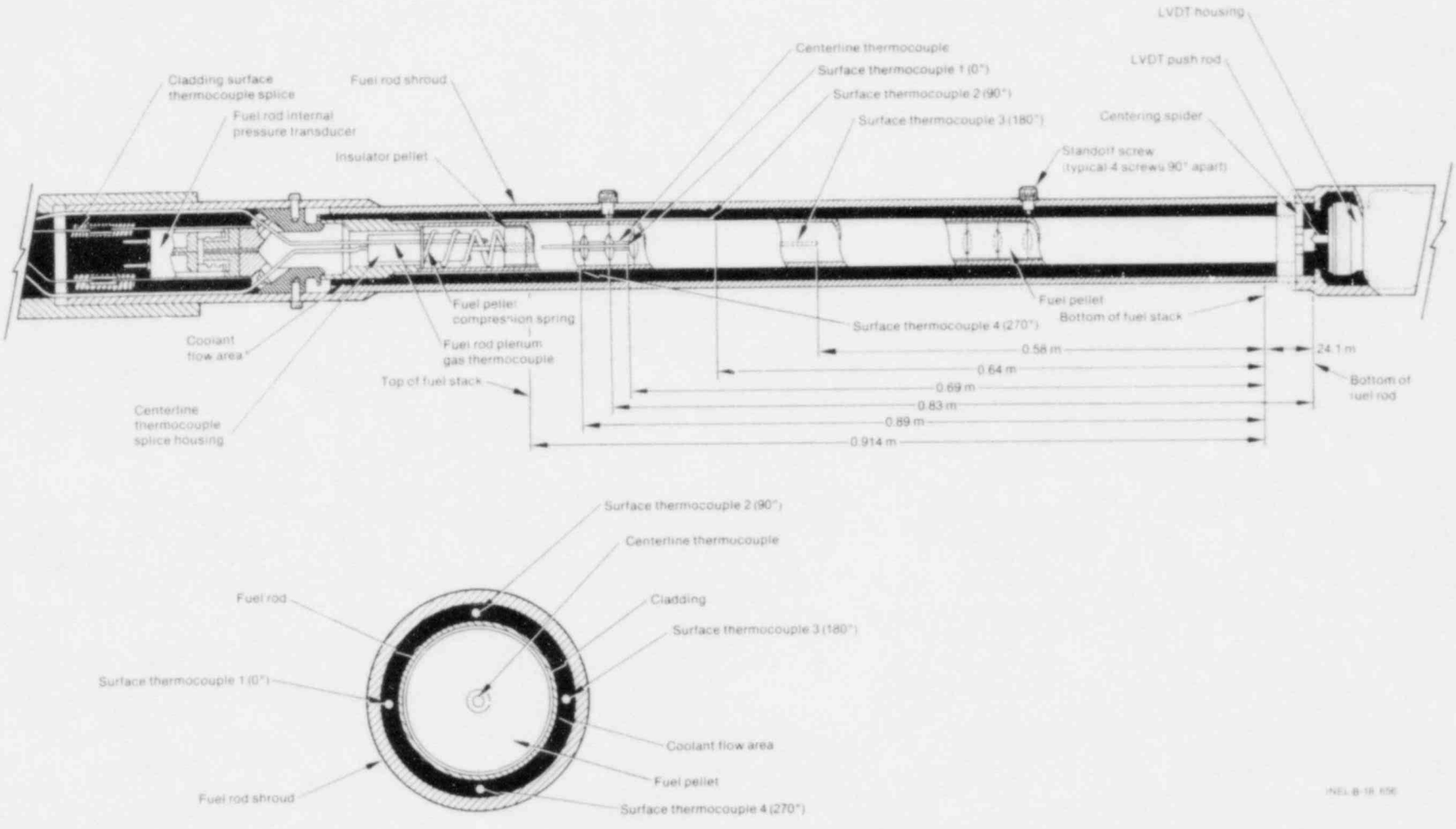

Figure 1. Typical PCM and IE test fuel rod and instrumentation shown installed in its flow shroud.

50 K/s, and the quenching rates were approximately 100 K/s down to the reactor ambient coolant temperature of ~600 K. The PCM test rods were subjected to film boiling conditions for time periods ranging from a few seconds to about 15 minutes, with cladding peak temperatures ranging from 1315 to ≥2100 K. The rods, following testing, were cooled in-pile to room temperature at a rate of approximately 0.02 K/s prior to their removal from the in-pile test loop.

2.4 Rod Damage Characterization

The mechanical behavior of the cladding is modified by both the beta-to-alpha phase transformation and oxidation processes. The typical effects of high-temperature film boiling are shown in Figure 2. Regions of surface oxide (ZrO_2) growth, oxide spalling that exposes the shiny base-metal zircaloy, and collapse of the cladding into fuel pellet-to-pellet interfaces along the film boiling zone are indicated. An example of the typical microstructures observed in zircaloy cladding that was oxidized under film boiling conditions for about 116 s is shown in Figure 3. Microstructural features such as outer single-layer surface oxide (ZrO_2), outer and inner layers of oxygen-stablized alpha-zircaloy, and the prior beta field are illustrated. Reaction layer development at the fuel-cladding interface is also evident in the figure.

2.5 Interpretation of In-Pile Embrittlement Data

Oxygenation from zircaloy-water reaction (at the exterior cladding surface) and zircaloy-UO_2 reaction (at the interior cladding surface) occur during film boiling operation and influence the cladding ductility. At temperatures above ~1100 K, the reaction of zircaloy with steam at the cladding outer surface produces a layer of zirconium oxide (ZrO_2) and a layer of oxygen-stablized α-zircaloy. The fuel-cladding interaction results in a layer of oxygen-stablized α-zircaloy of a thickness similar to the layer formed on the outer surface of the cladding. These results suggest that oxygen enters the cladding at about the same rate from both surfaces. Thus, the embrittlement resulting from film boiling operation in the PBF should be approximately comparable with that obtained in a two-sided reaction with steam (out-of-pile experiments). Effective isothermal temperatures were determined for the PBF test rods in order to compare embrittlement criteria developed from out-of-pile isothermal tests with the in-pile results. The effective isothermal temperature is the temperature that accounts for the growth of the cladding exterior surface reaction layers (ZrO_2 and oxygen-stablized α-zircaloy) for the film boiling time of the experiment.[6] From measurements of cladding exterior surface reaction layer thicknesses and experimental film boiling times, and using zircaloy oxidation kinetics,[31] the effective isothermal temperatures were calculated as described in Reference 32 with an estimated uncertainty of ±50 K. The difference between the peak cladding temperature calculated by the modified COBILD computer code and the effective isothermal temperature had values that varied up to about 350 K.[4] The film boiling times obtained from in-pile measurements of cladding surface temperatures and fuel rod axial expansion were adjusted to a reference value of wall thickness. Film boiling time, cladding temperature, fractional thickness of transformed β phase (F_W), thickness of the β phase containing ≤0.9 wt% oxygen [$L_{\beta(0.9)}$], thickness of the β phase containing ≤0.7 wt% oxygen [$L_{\beta(0.7)}$], and equivalent cladding reacted (ECR) were obtained at locations adjacent to the fractures, while for rods that did not fracture, these data were obtained at locations of maximum cladding temperature determined by metallographic examination. In addition, the cladding hydrogen content was measured by vacuum fusion mass spectrometry at those same locations.

The main difficulty in comparing the out-of-pile data with the in-pile data arises from the fact that the out-of-pile experiments are conducted under controlled isothermal oxidation conditions while the in-pile oxidation conditions vary widely depending on the film boiling transients. The rate of oxygen diffusion increases significantly at temperatures above 1100 K. Based on this variance and given a difference between the isothermal effective cladding temperature and the peak cladding temperature for the in-pile tests that could be as high as 350 K, some discrepancies in comparisons of the in-pile and out-of-pile data could be expected.

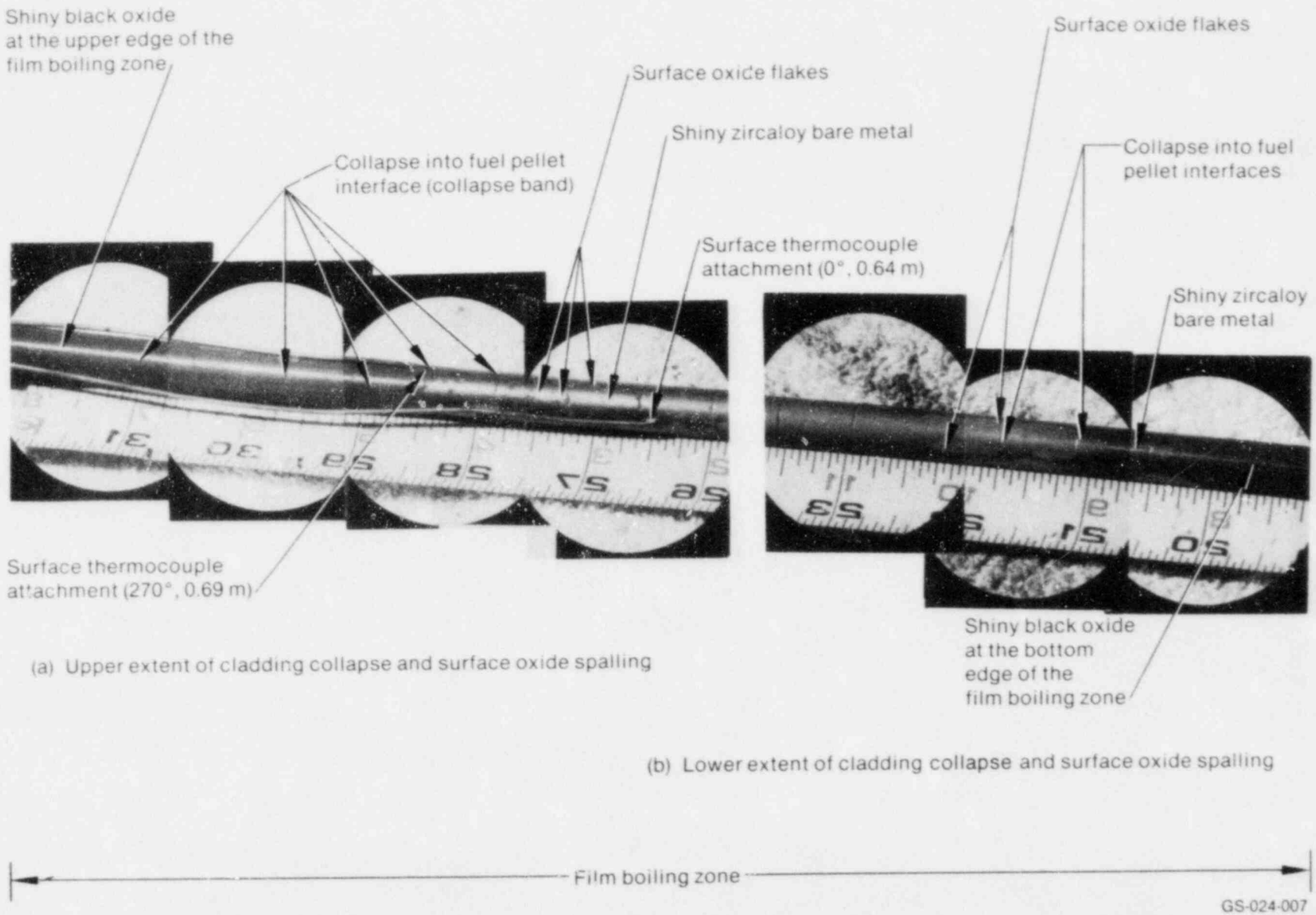

Figure 2. Film boiling zone on Rod UTA-008 (0-to-270-degree orientation).

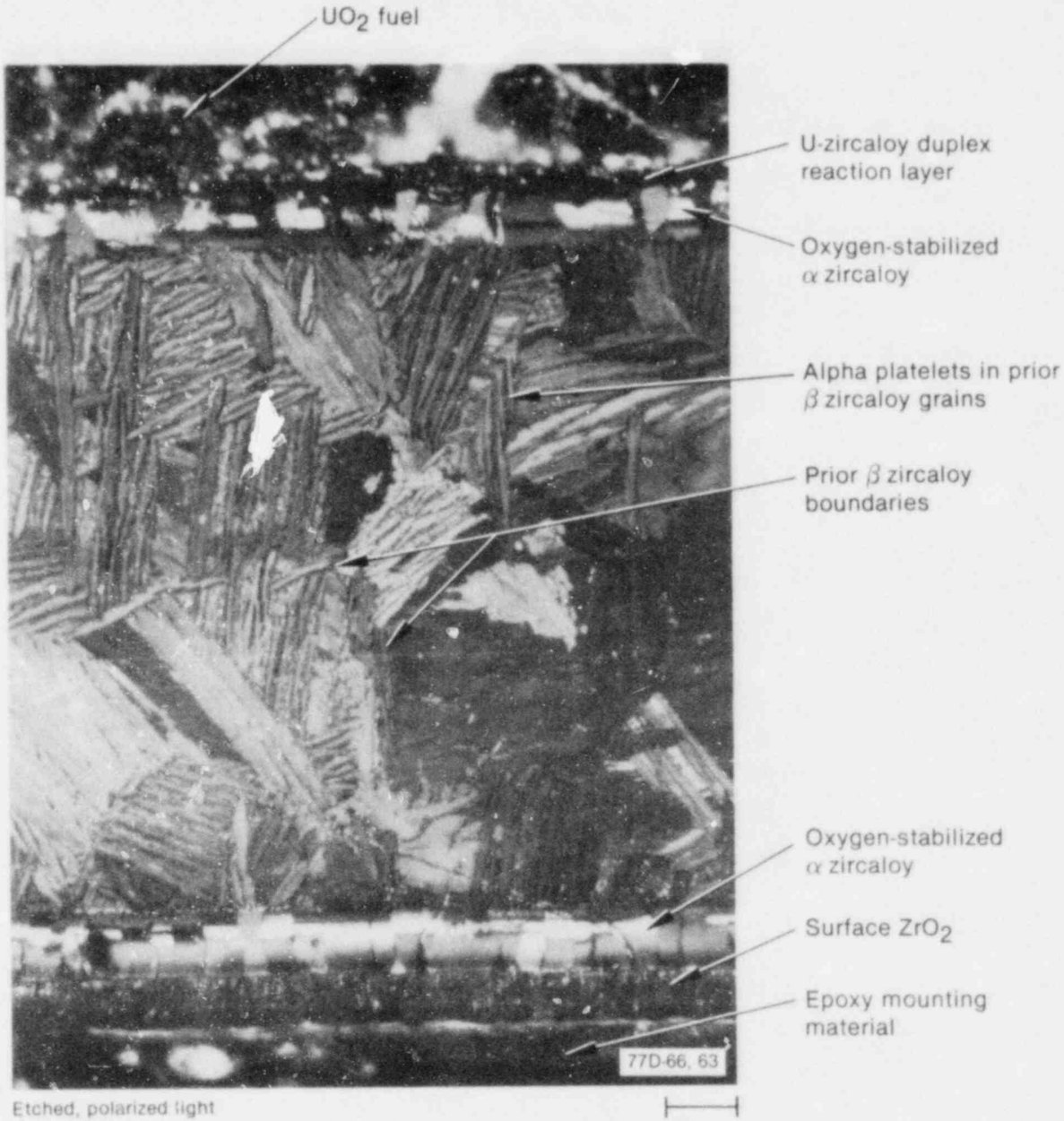

Figure 3. Photomicrograph showing the cladding microstructure of a fuel rod that experienced film boiling operation (longitudinal section from Rod UTA-0017 between 0.629 and 0.648 m from bottom of fuel stack).

Table 1. Embrittlement parameters of the PBF tests.

Rod Number	Cladding	Fuel	Pretest Cladding Wall Thickness (mm)	Exposure Time in Film Boiling (s)	Isothermal Effective Cladding Temperature (K)	Elevation From Bottom of Fuel Stack (m)	F_w (%)	Equivale Claddin Reacted (%)
UTA-0004	Unirradiated	Unirradiated	0.61	345	1740	0.576[a]	3	27
UTA-0004	Unirradiated	Unirradiated	0.61	260	1575	0.505[a]	54	11
UTA-0005	Unirradiated	Unirradiated	0.61	39	1410	0.567	93	2
UTA-0006	Unirradiated	Unirradiated	0.61	78	1450	0.768	97	2
UTA-0007	Unirradiated	Unirradiated	0.61	180	1480	0.663	79	6
UTA-0008	Unirradiated	Unirradiated	0.61	101	1600	0.533	71	7
A-0014	Unirradiated	Unirradiated	0.61	57	1450	0.623	90	3
A-0015	Unirradiated	Unirradiated	0.61	17	1640	0.483	84	4
A-0021	Unirradiated	Unirradiated	0.61	26	1580	0.425[a]	88	6
UTA-0014	Unirradiated	Unirradiated	0.61	55	1475	0.600	87	4
UTA-0015	Unirradiated	Unirradiated	0.61	67	1625	0.606	72	7
UTA-0016	Unirradiated	Unirradiated	0.61	136	1490	0.667	78	6
UTA-0017	Unirradiated	Unirradiated	0.61	116	1505	0.629	78	5
IE-001	Unirradiated	Unirradiated	0.59	70	1690	0.482	57	12
IE-001	Unirradiated	Unirradiated	0.59	288	1630	0.597[a]	41	17
IE-005	Irradiated	Unirradiated	0.59	37	1410	0.794	94	2
IE-007	Irradiated	Irradiated	0.59	48	1860	0.501[a]	22	24
IE-008	Irradiated	Irradiated	0.59	20	1540	0.559	90	3
IE-009	Irradiated	Irradiated	0.59	60	1270	0.565	93	2
IE-010	Irradiated	Irradiated	0.59	79	1640	0.559	56	7
IE-011	Irradiated	Unirradiated	0.62	94	1760	0.592	75	11
IE-012	Irradiated	Unirradiated	0.62	75	1380	0.580	92	2
IE-013	Unirradiated	Unirradiated	0.59	87	1520	0.592	75	8
IE-014	Unirradiated	Unirradiated	0.59	91	1440	0.598	85	6
IE-015	Irradiated	Irradiated	0.59	84	1750	0.584[a]	47	16
IE-016	Irradiated	Irradiated	0.59	36	1920	0.539[a]	45	17
IE-017	Irradiated	Irradiated	0.59	71	1540	0.578	78	6
IE-018	Irradiated	Irradiated	0.59	78	1620	0.595	63	9
IE-019	Irradiated	Unirradiated	0.60	44	1700	0.502[a]	73	9
IE-019	Irradiated	Unirradiated	0.60	44	1590	0.571[a]	82	8
IE-019	Irradiated	Unirradiated	0.60	76	1535	0.625[a]	74	12
IE-020	Irradiated	Unirradiated	0.60	56	1700	0.568	58	10
IE-021	Irradiated	Unirradiated	0.61	31	1840	0.527[a]	62	10
IE-022	Unirradiated	Unirradiated	0.61	31	1940	0.495[a]	50	16

Remaining Prior β Thickness (mm)	$L_{\beta(0.9)}$[g] (mm)	$L_{\beta(0.7)}$[h] (mm)	Cladding Gas Sample Elevation from Bottom of Fuel Stack (m)	Hydrogen Content (ppm H_2)	Comments
0.020	0.000	--	--	--	Rod failed in-pile 60 s after shutdown
0.317	--	0.255	--	--	Rod failed in-pile and fractured during posttest handling
0.570	0.575	0.551	--	--	Intact rod
0.591	0.590	0.569	--	--	Intact rod
0.471	0.523	0.457	--	--	Intact rod
0.430[b]	0.422	0.373	--	--	Intact rod
0.553[c]	0.572	0.534	--	--	Intact rod
0.502	0.517	0.490	--	--	Intact rod
0.509	--	0.488	0.441	340	In-reactor breach, and fracture during posttest handling
0.530[b]	0.549	0.519	--	--	Intact rod
0.426	0.446	0.393	--	--	Intact rod
0.460	0.491	0.449	0.667	50	Intact rod
0.462	0.509	0.456	0.797	180	Intact rod
0.337[b]	0.367	0.311	--	--	Intact rod
0.231	0.069	--	--	--	Rod failed in-pile 80 s after shutdown
0.554	0.565	0.565	--	--	Intact rod
0.140	0.000	--	--	--	Rod failed in-pile 180 s after shutdown
0.530	--	--	--	--	Rod breached in-pile due to massive hydriding[d]
0.553	0.572	0.572	--	--	Intact rod
0.332[b]	0.407	0.347	--	--	Intact rod
0.468[b]	0.245	--	0.573	120	Intact rod
0.575	0.590	0.590	--	--	Intact rod
0.445[b]	0.508	0.460	0.573	50	Intact rod
0.505[b]	0.530	0.499	--	--	Intact rod
0.230	--	0.268	--	--	Rod failed during posttest handling
0.250	--	0.173	--	--	Rod failed during posttest handling
0.464[b]	0.492	0.440	0.571	390	Intact rod
0.375[b]	0.350	0.402	--	--	Intact rod
0.432	--	--	0.511	1020	In-reactor breach, and fracture during posttest handling
0.472	--	0.365	--	--	In-reactor breach, and fracture during posttest handling
0.410	--	0.419	--	--	In-reactor breach, and fracture during posttest hand'ing
0.337	0.389	0.337	0.543	40	Intact rod
0.367	--	0.293	0.514	60	Rod failed in-pile 90 s after shutdown, and handling fracture
0.310	--	0.242	0.482	300	Rod failed in-pile 90 s after shutdown, and handling fracture

Table 1. (continued)

Rod Number	Cladding	Fuel	Pretest Cladding Wall Thickness (mm)	Exposure Time in Film Boiling (s)	Isothermal Effective Cladding Temperature (°)	Elevat Fro Botto of Fu Stac (m)
201-1	Unirradiated	Unirradiated	0.61	895	1690	0.67
205-1	Unirradiated	Unirradiated	0.62	665	1700	0.58
205-3	Unirradiated	Unirradiated	0.62	165	1500	0.68
205-4	Unirradiated	Unirradiated	0.62	--	1850	0.68
205-5	Unirradiated	Unirradiated	0.62	135	1540	0.68
205-6	Unirradiated	Unirradiated	0.62	45	1300	0.78
205-8	Unirradiated	Unirradiated	0.62	310	1750	0.68
207-1	Unirradiated	Unirradiated	0.61	250	1570	0.62
207-2	Unirradiated	Unirradiated	0.61	1600	1600	0.53
207-3	Unirradiated	Unirradiated	0.61	440	1650	0.62
207-4	Unirradiated	Unirradiated	0.61	1400	1600	0.68
207-5	Unirradiated	Unirradiated	0.61	1640	--[f]	--
207-6	Unirradiated	Unirradiated	0.61	1160	1540	0.55

a. Fracture location.

b. The width of the remaining phase was determined on the basis of the original

c. Cladding samples analyzed were taken from rod fragments within the high-power r

d. Failure not attributed to PCM conditions.

e. Value of the content was estimated metallographically.

f. Failed section of fuel rod broke away from the fuel rod in-pile and was missing.

g. $L_{(0.9)}$ = Beta-phase thickness containing 0.9 wt% oxygen (mm).

h. $L_{(0.7)}$ = Beta-phase thickness containing 0.7 wt% oxygen (mm).

ion m el k	F_w (%)	Equivalent Cladding Reacted (%)	Remaining Prior β Thickness (mm)	$L_{\beta(0.9)}$ [g] (mm)	$L_{\beta(0.7)}$ [h] (mm)	Cladding Gas Sample Elevation from Bottom of Fuel Stack (m)	Hydrogen Content (ppm H_2)	Comments
	1	24	0.0[b]	--	--	[c]	360	In-pile breach and failure during film boiling
	1	28	0.0[b]	--	--	--	--	Rod failed in-pile at 500 s in film boiling
	75	7	0.437[b]	--	--	0.68	50[e]	Intact rod
	61	10	0.387[b]	--	--	0.68	43	Rod failed during posttest handling
	74	7	0.466[b]	--	--	0.68	29	Intact rod
	90	2	0.559[b]	--	--	--	--	Intact rod
	16	21	0.110[b]	--	--	--	--	Rod failed in-pile at 250 s in film boiling
	94	5	0.420	0.495	0.438	--	--	Intact rod
a	0.0	100	0.0	0.0	--	--	--	Rod failed in-pile
a	0.0	100	0.0	0.0	--	--	--	Rod failed in-pile
a	0.0	100	0.0	0.0	--	--	--	Rod failed in-pile
	--[f]	--[f]	--[f]	--[f]	--[f]	--	--	Rod failed in-pile
	0.0	100	0.0	0.0	--	--	--	Rod failed in-pile

all thickness.

gion of the test rod.

during posttest examination.

vendor analysis of loss-of-coolant accident (LOCA) design-basis accidents. ECR is equivalent to using the total oxygen content in the product reaction layers to determine the fraction of the zircaloy wall thickness capable of being completely oxidized to ZrO_2. Scatena[33] presented a relationship between ECR and the product reaction layers of the form

$$\% \text{ ECR} = \frac{100}{W} \times \left[\frac{\text{Oxide thickness}}{1.54} + \frac{\text{Alpha thickness}}{1.54\sigma} \right] \quad (3)$$

where W is the cladding wall thickness, 1.54 is the oxide-to-metal molar volume ratio for ZrO_2/Zr, and σ is the ratio of the weight fraction of oxygen in ZrO_2 to the average weight fraction of oxygen in the stabilized alpha phase. The factor σ was determined by using the zirconium-oxygen constitutional equilibrium phase diagram and assuming the oxygen concentration in the alpha phase to be a linear average between the oxygen content at the alpha/alpha + beta and the alpha/alpha + ZrO_2 boundaries for each effective cladding temperature. In Equation (3) the total oxygen uptake is assumed to equal the oxygen contained in the surface oxide layers and the two-sided oxygen-stabilized alpha product layers. The oxygen content in the beta phase was assumed to be negligible.

The in-pile test data compiled in Table 1 are presented in Figures 6 and 7 where the % ECR is plotted as a function of the effective isothermal cladding temperature for thermal shock and handling failures, respectively. The ANL out-of-pile data (cladding samples oxidized for <900 seconds) are plotted on the same figures. The dotted lines in the two figures represent the threshold limit of 17% suggested by Scatena. The out-of-pile thermal shock failures presented in Figure 6 occurred at values of ECR ≥20%; a number of out-of-pile samples did not fail even with ECR values near 30%. Thus, the in-pile quenching failures are predictable by the 17% ECR criterion. All the in-pile handling failures and one out-of-pile handling failure are not predictable by Scatena's 17% ECR criterion, as shown in Figure 7. Thus, this criterion, although not applicable to handling failures, predicts thermal shock (quench) failures.

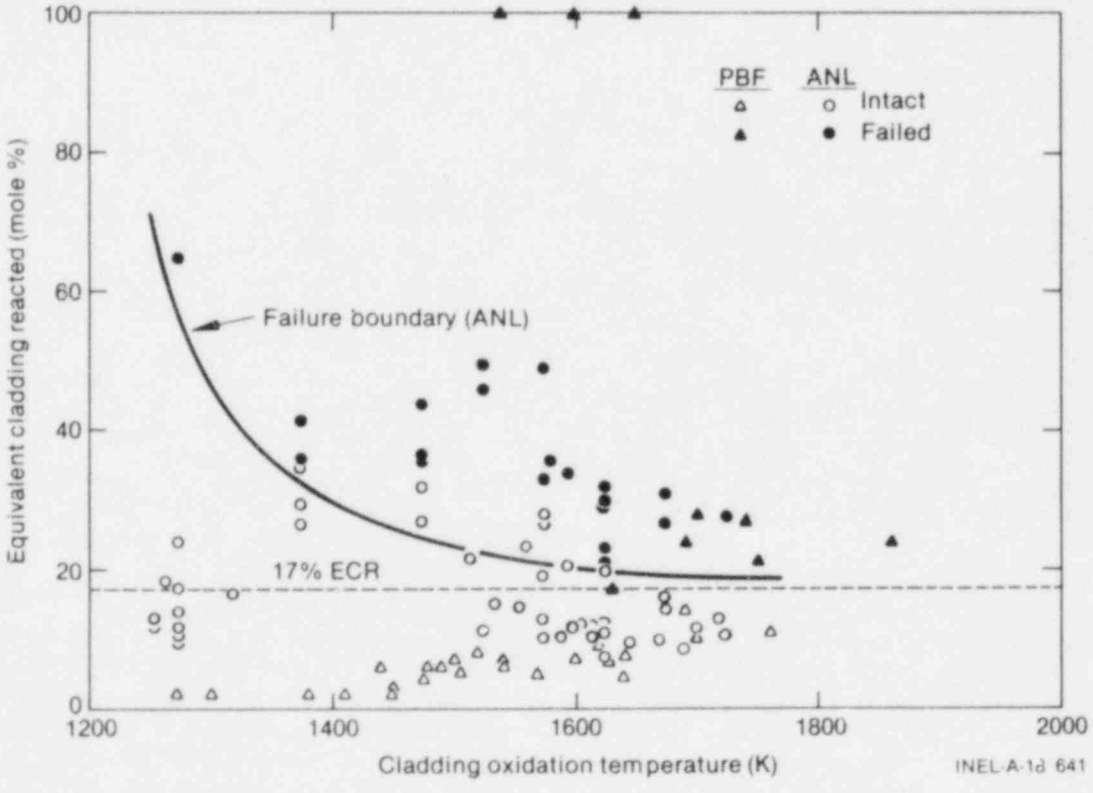

Figure 6. Equivalent cladding reacted, plotted as a function of temperature (thermal shock data).

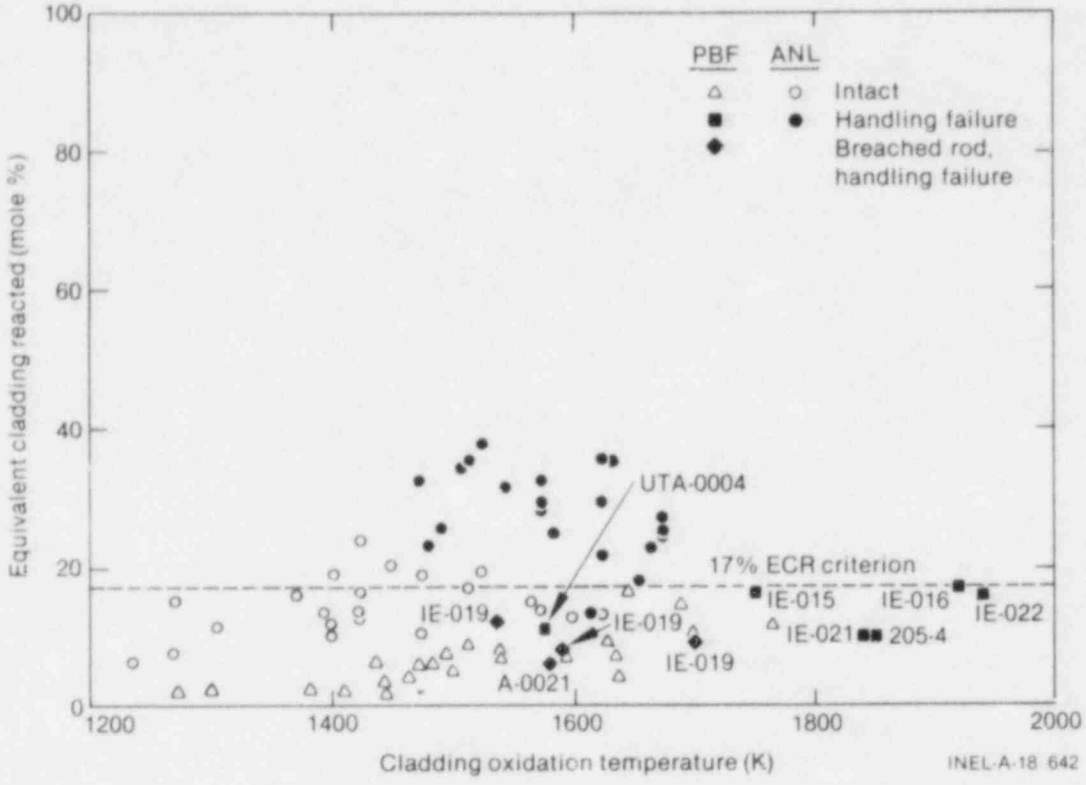

Figure 7. Equivalent claddin reacted, plotted as a function of temperature (handling failure data).

3.3 Oxygen Content in the Beta Phase

Oxidation of the zircaloy cladding increases the oxygen content in the remaining beta phase. The oxygen content in the beta phase was used as a measure of the overall room-temperature embrittlement.

An embrittlement criterion suggested by Chung and Kassner[2] states that the calculated thickness of the cladding with ≤0.9 wt% oxygen, $L_{\beta(0.9)}$, based on the average wall thickness at any axial location, should be greater than 0.1 mm in order for the cladding to withstand thermal shock during a LOCA reflood. The ANL out-of-pile experimental data are presented in Figure 8 together with the PBF data, where the thickness of the beta phase containing ≤0.9 wt% oxygen is plotted as a function of temperature (the isothermal oxidation temperature and the effective isothermal cladding temperature for the ANL and PBF data, respectively). The criterion is represented on Figure 8 by the dotted line. The criterion of $L_{\beta(0.9)}$ >0.1 mm accounted for the thermal shock failures in the PBF and all but one of the out-of-pile failures.

The second criterion suggested by Chung and Kassner[2] for the capability of the cladding to withstand posttest handling failures (based on 0.3J impact failure limit), states that the thickness of the cladding with ≤0.7 wt% oxygen, $L_{\beta(0.7)}$, should be greater than 0.3 mm, based on the average wall thickness at any axial location. The PBF and ANL data presented in Figure 9 show the predictability of cladding handling failures according to the Chung and Kassner embrittlement criterion. Three of the handling failures not predicted by the criterion occurred in rods that operated with breached cladding during film boiling testing (Rods A-0021 and IE-019). These claddings contained a modified prior beta phase and were anomalously embrittled.[7] In addition, these claddings were found to have hydrogen contents of 340 and 1020 ppm after testing.

In an earlier work (References 4 and 7) the PBF data were compared with Chung and Kassner embrittlement criteria, using average oxygen concentrations in the beta phase. However, the oxygen profile in the beta phase should be used to obtain an exact comparison. Since the computer code COBILD, did not accurately calculate the oxygen profile for the earlier work, it was modified for the

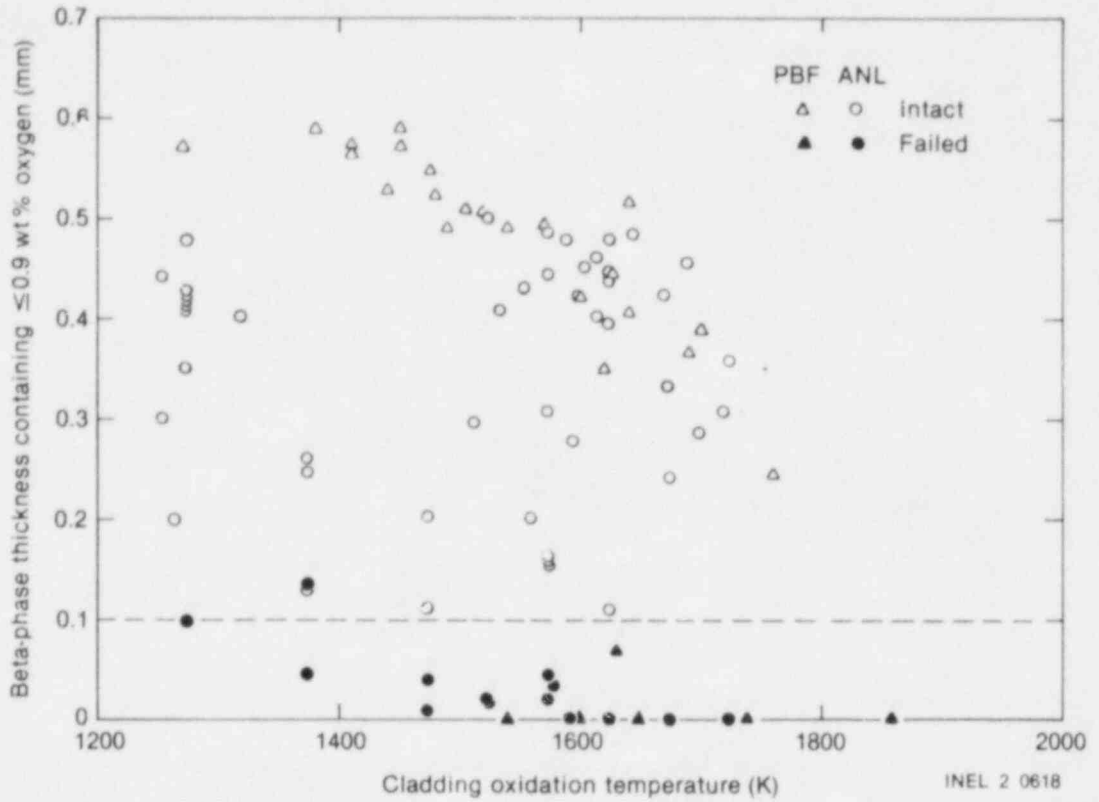

Figure 8. Failure map for zircaloy-4 cladding by thermal shock relative to wall thickness with ≤0.9 wt% oxygen.

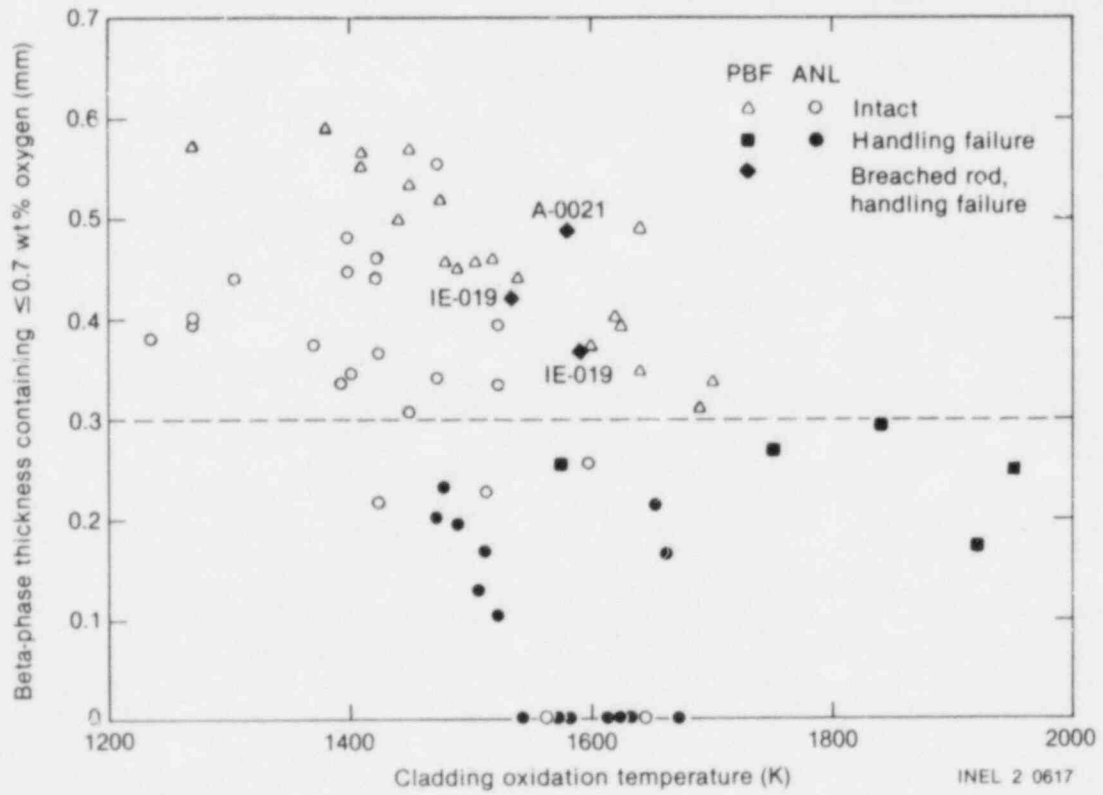

Figure 9. Failure map for zircaloy-4 cladding due to handling relative to wall thickness with <0.7 wt% oxygen.

PBF tests. The modified code is reported in Reference 5. The code listing is given in Appendix B. Although this code considers only one-sided cladding oxidation, the results indicate the applicability of Chung and Kassner criteria to the PBF data. The driver of the COBILD code (provided in Appendix B) allows the user to run the code with an increasing temperature multiplication factor in steps determined by the user until the thickness of a predefined layer [ZrO_2 layer, α layer, or the ξ layer (ZrO_2 + α)] matches the measured thickness of the corresponding layer. If the oxide layer were partially or completely spalled off, the user would run the COBILD code with the driver specifying comparison of the calculated alpha layer with the measured one. This was the case for a few of the PBF fuel rods. In addition, the orientation of the PBF fuel rod specimens containing the maximum oxide or α-layer thickness was chosen for the analysis. That choice was made since large circumferential temperature differences of the PBF fuel rods produced various amounts of oxygen uptake in the cladding at different orientations for the same elevation. Consequently, it should be noted that the accuracy in measuring the thickness of the oxide and α layers in oxidized cladding, as well as the appropriate setting of the driver of the COBILD code, are very important requirements for determining the zircaloy cladding embrittlement.

As previously mentioned, oxygen profiles in the remaining beta phase of the zircaloy cladding tested in-pile were calculated with the COBILD code using temperature histories of the transients and by assuming only one-sided oxidation of the cladding. However, oxygen profiles of the zircaloy beta phase in the ANL out-of-pile tests were calculated based on isothermal-temperature, two-sided cladding oxidation.[2] Since the COBILD code does not model two-sided cladding oxidation, the following simple, conservative approach, illustrated in Figures 10-12, was tried for Rods IE-019 (samples I-1 and I-2) and A-0021 to investigate the applicability of Chung and Kassner's criterion for handling failures to these rods that operated with breached cladding during film boiling testing. In Figures 10-12, the dotted line represents the oxygen concentration profile in

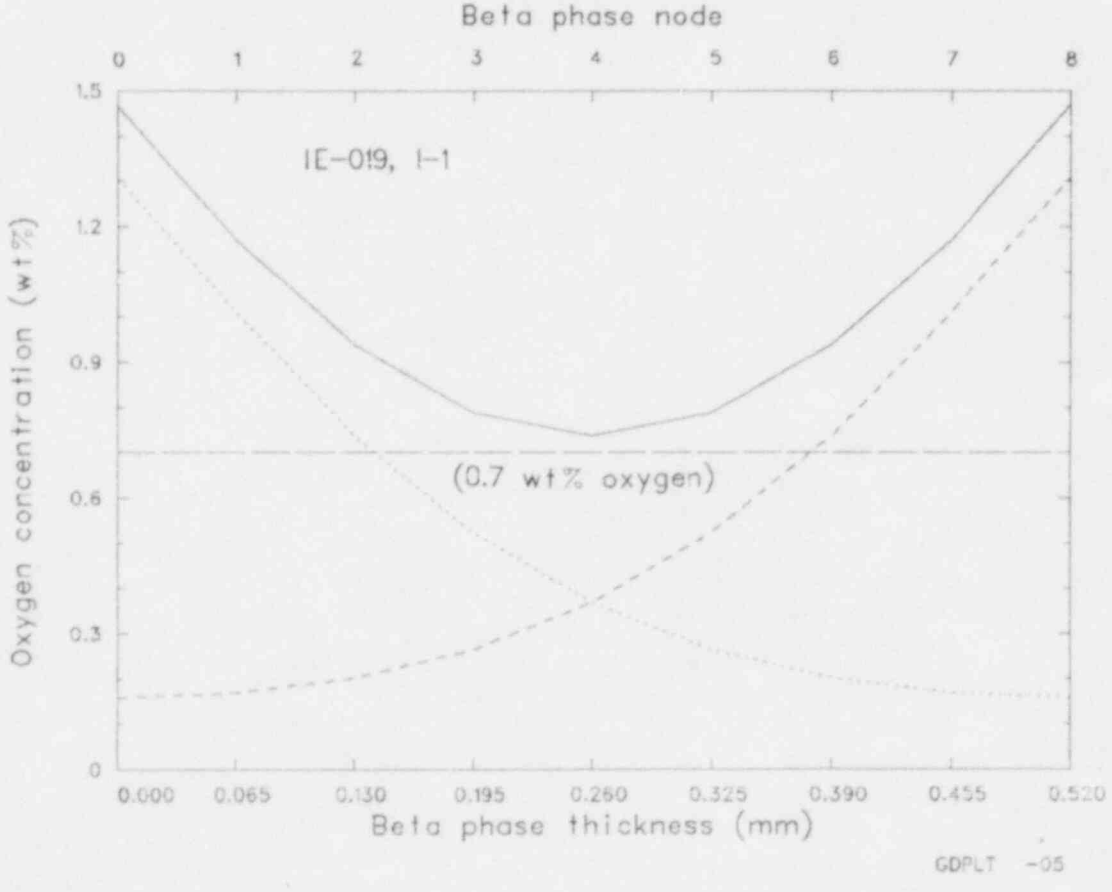

Figure 10. Oxygen concentration in the zircaloy beta-phase at 0.571-m elevation of Rod IE-019, sample I-1.

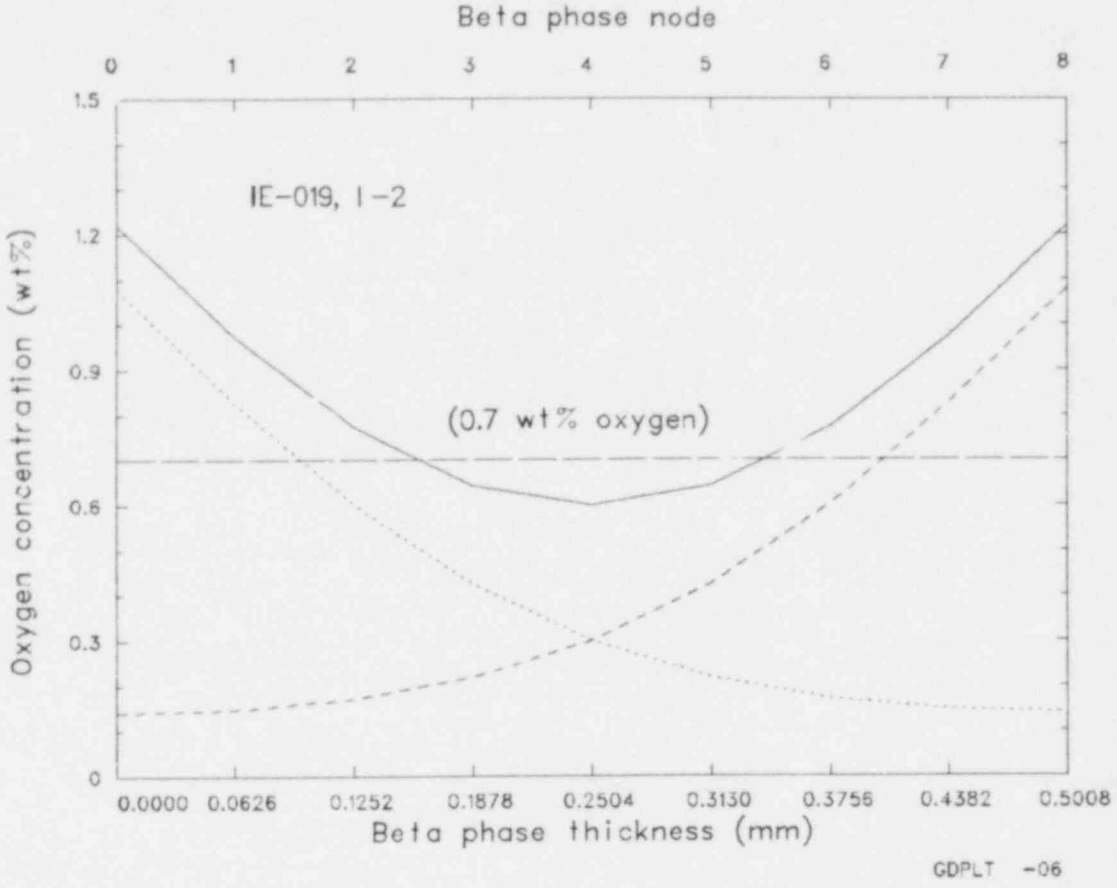

Figure 11. Oxygen concentration in the zircaloy beta-phase at 0.625-m elevation of Rod IE-019, sample I-2.

the cladding beta phase. That profile was calculated with the COBILD code at 9 nodes where node 0 is near the cladding outer surface. The dashed line is a mirror image of the dotted line, indicative of oxidation from the cladding inside surface. The solid line is the summation of both the dotted and dashed lines. The latter is representative of two-sided oxidation, but it is conservative since oxidation on each side, calculated with the COBILD code, is obtained by assuming oxygen diffusion in an infinite thickness of zircaloy cladding. Oxygen concentration profiles due to two-sided oxidation would be lower, considering a finite thickness of the cladding changes the oxygen diffusion kinetics, which in turn results in less oxygen uptake in the cladding. Calculations based on these solid lines indicated that the handling failures of Rod IE-019 are predictable [$L_{\beta(0.7)} = 0.0$ mm and $L_{\beta(0.7)} = 0.183$ mm for samples I-1 and I-2, respectively], while the handling failure of Rod A-0021 is still not predicted [$L_{\beta(0.7)} = 0.363$ mm]. More detailed experimental investigation of the fracture locations of these rods (IE-019 and A-0021) using the following techniques would explain the anomalous embrittlement of these rods: optical microscopy, scanning electron microscopy (to obtain some fractographs), scanning auger microscopy (to map oxygen distribution as well as to obtain the profile of oxygen concentration), vacuum fusion mass spectrometry (to measure the hydrogen uptake in the cladding), and microhardness testing.

3.4 Failure Boundary Based On Time-at-Oxidation Temperature

Failure boundaries for thermal shock are shown on a plot of oxidation time versus oxidation temperature in Figure 13 for both in-pile and out-of-pile test data. The abscissa represents the inverse of both the isothermal oxidation temperature and the effective isothermal cladding temperature for the out-of-pile and in-pile data, respectively. The ordinate represents the time at oxidation temperature and the time in film boiling (adjusted to the ANL reference

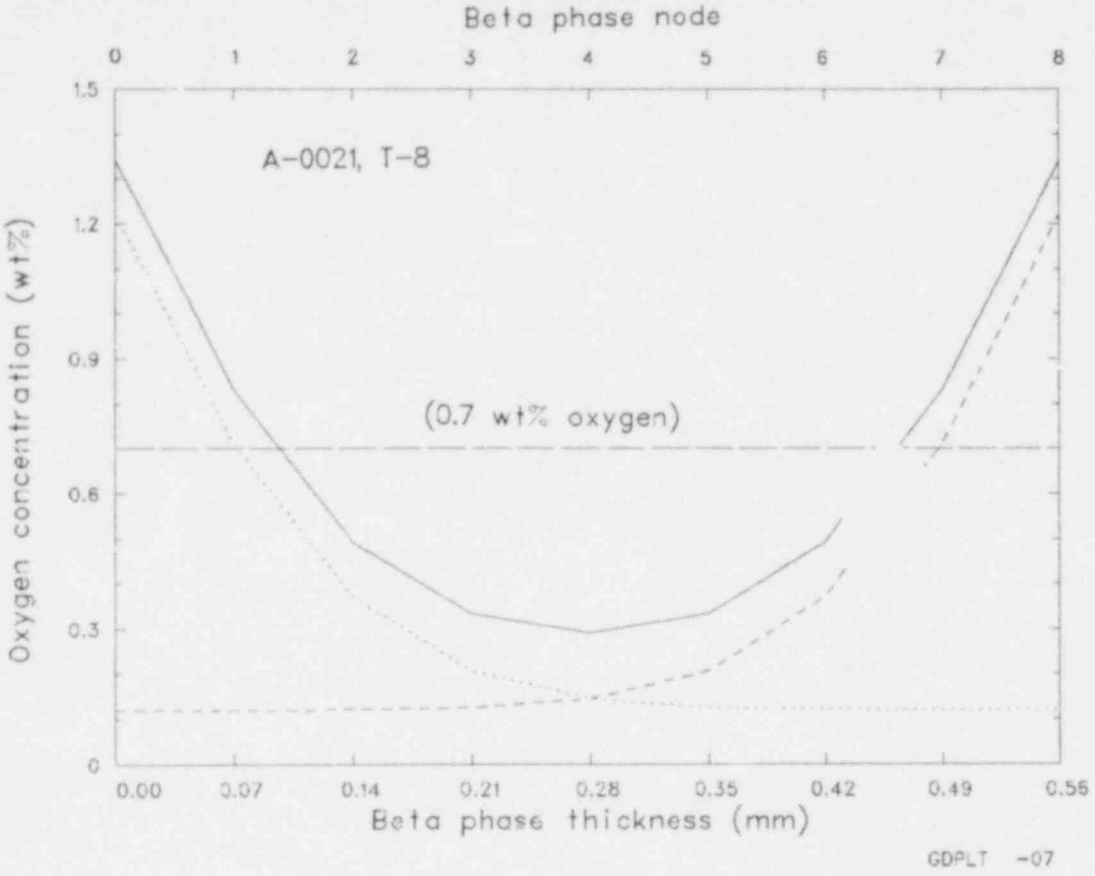

Figure 12. Oxygen concentration in the zircaloy beta-phase at 0.425-m elevation of Rod A-0021, sample T-8.

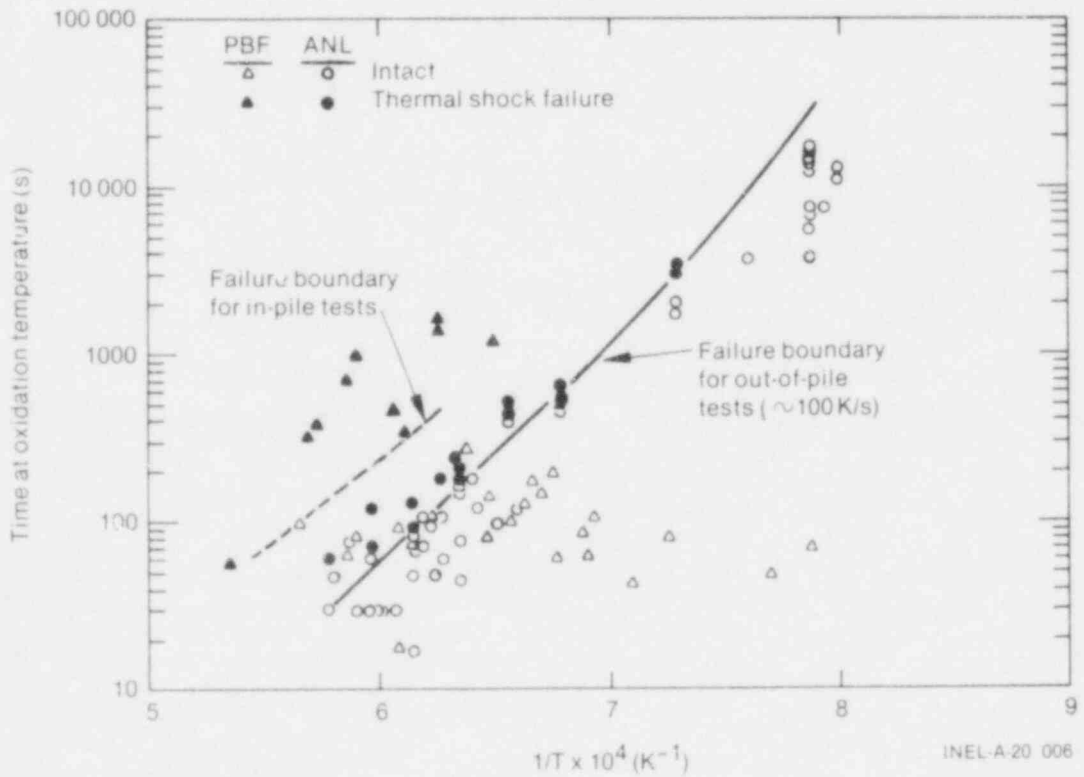

Figure 13. Failure boundaries of thermal shock for in-pile and out-of-pile tests.

cladding thickness by multiplying by the ratio $\left[\frac{0.635\ \text{mm}}{\text{pretest PBF cladding thickness in mm}}\right]^2$ for the out-of-pile and the PBF data, respectively.

The solid and dashed lines in Figure 13 are the thermal shock failure boundaries for the out-of-pile and in-pile experiments, respectively. It can be seen from this figure that the failure boundary for the out-of-pile tests is more conservative (permits less oxidation time at a given oxidation temperature) than the in-pile failure boundary.

Pawel[34] has suggested the values of 0.7 wt% for the mean oxygen concentration in the beta phase, together with a 95% saturation condition as critical criteria for the onset of room temperature embrittlement. The calculated time required at a given temperature to exceed either of the Pawel's values is shown by the two solid curves in Figure 14. In this figure, both the PBF and the ANL out-of-pile data are presented for adjusted times up to 1100 s. The whole field of data for the PBF and the ANL tests is shown on a semilog plot in Figure A-1 of Appendix A. In addition, these data are presented in Tables A-1 and A-2 of Appendix A. The film boiling times for the PBF tests and the times of isothermal oxidation temperatures for the ANL tests were adjusted to the reference cladding thickness of 0.686 mm by

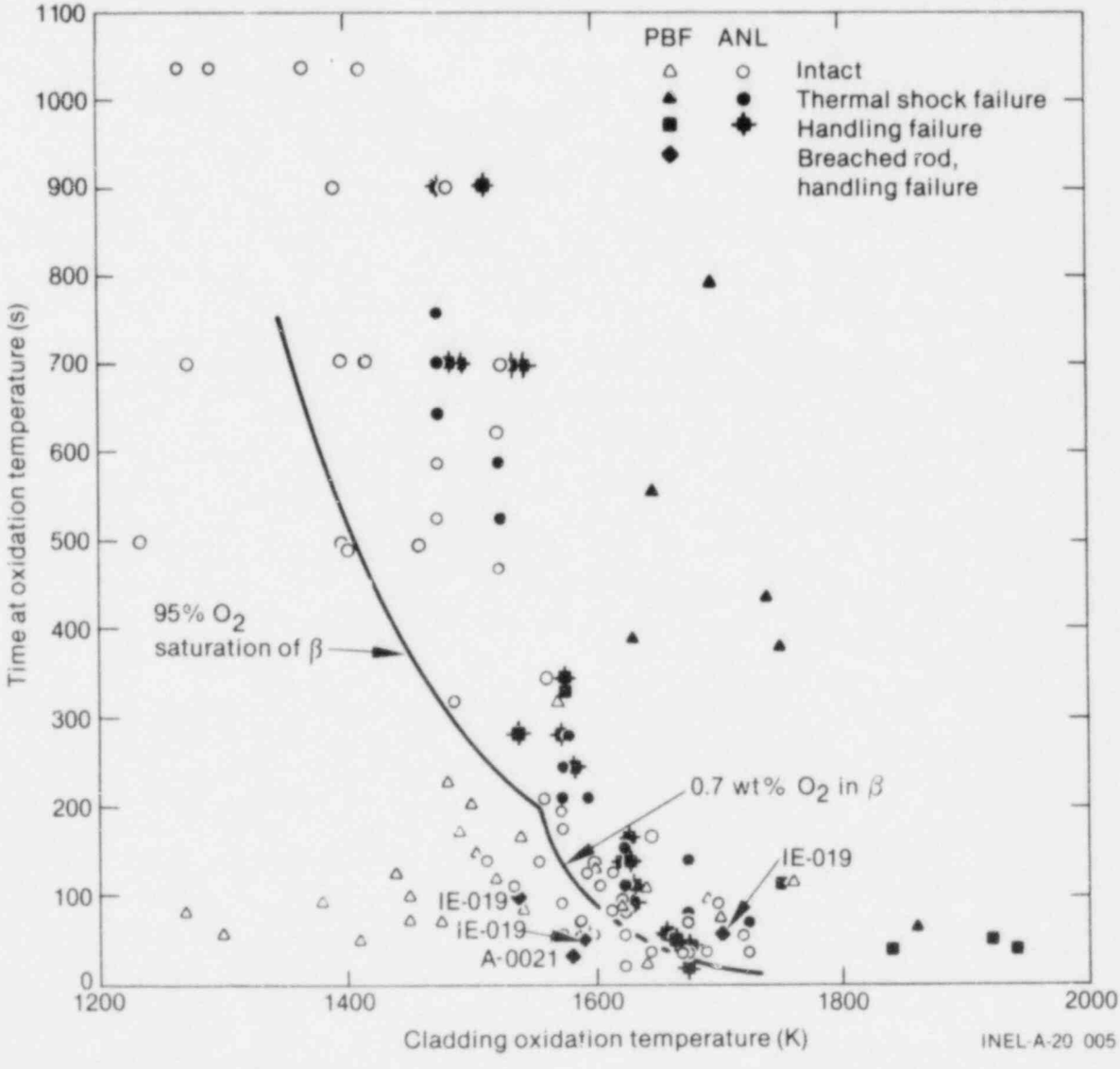

Figure 14. Failure map for the in-pile (PBF) and the out-of-pile (ANL) tests.

multiplying each time by the correction factor of [0.686 mm/original cladding wall thickness]^2 to bring the data to the same cladding thickness basis used in the Pawel's analysis.

The limiting conditions for embrittlement defined by Pawel account for all but one out-of-pile fracture and three in-pile fractures. However, Pawel's criteria do not distinguish the cause of rod failure (quenching or handling). The three PBF fractures are from the two test rods (Rods A-0021 and IE-019) that operated in film boiling during testing with breached cladding, and fractured during posttest handling. The data for the ANL rod (test number BSF-1363), which was isothermally oxidized at 1673 K for an adjusted time of 23 s and fractured at an impact energy of 0.03 J, plots very close to the 0.7 wt% oxygen criterion. This data point suggests that this criterion is not in significant disagreement with this out-of-pile handling failure. Some intact rods from both in-pile and out-of-pile tests were found in the region of the plot where failures would be expected. Ring ductility tests on samples from two intact PBF rods that were predicted to be brittle (Rods IE-010 and IE-020) indicated 2% and 0% ductility, respectively. The ECR values for these samples, 16% and 10%, respectively, are well within the 17% criterion, but the samples exhibited little or no ductility.

3.5 Anomalous Microstructural Effects Influencing Embrittlement

Several microstructural features relating to a loss-of-fracture resistance of oxidized cladding have been identified.[7] The features are characterized in the following subsections.

3.5.1 Beta-Phase Grain Boundary Alpha. The embrittlement of Rods A-0021 and IE-019 was not predicted by any of the embrittlement criteria discussed. Rod A-0021 apparently failed during testing (probably due to a fabrication defect), and Rod IE-019, a high-pressure rod, ballooned to failure early in the high-temperature transient.[35] The cladding of both rods was breached within the film boiling zone during transient operation, permitting access of the coolant steam to the rod interior. Each of these rods arrived at the hot cell intact, but fractured during subsequent normal remote handling.

The failure of Rod IE-019 during the film boiling transient was detected by the rod internal pressure transducer. Rod A-0021 did not contain a device for measuring its internal pressure. The thickness of the ZrO_2 layer found on the inner surface of the cladding of Rod A-0021 was similar to that on the exterior surface. This observation strongly suggests that the rod contained a fabrication defect or failed early in the test due to a multiplicity of high-temperature cycles, and was operated during the last temperature transient with access of steam to the rod interior. The breach in the cladding was so small that it was not visually detectable prior to the rod handling fracture.

The operation of Rods A-0021 and IE-019 in film boiling with access of steam to the rod interiors resulted in the formation of unique cladding microstructural features. As shown in Figures 15 and 16, these features are extensive precipitation of α-zircaloy in prior beta grain boundaries (rim α) and acicular precipitation of α-zircaloy within the prior beta grains. These microstructures are similar to one reported earlier by Hobson[36] to be anomalously brittle at an F_W value of 0.9. At the fractures in Rods A-0021 and IE-019, the F_W ranged from 0.73 to 0.88.

The rim alpha structures could be expected to promote intergranular fracture; however, as can be seen in Figures 15 and 16, the through-wall fractures in these photomicrographs appear to be predominantly transgranular. A scanning electron micrograph from Rod IE-019 of a replica of the cladding fracture surface transverse to the rod axis is presented in Figure 17. The overlapping (stepped) nature of the fracture surface in the prior beta field indicates preferential fracturing, perhaps along prior beta grain boundaries or hydride platelets.

3.5.2 Hydrogen. In laboratory experiments performed by Homma et al.,[37,38] the oxidation of breached cladding exposed to flowing steam only on the external surface resulted in more severe embrittlement than for intact cladding exposed to flowing steam on both sides. The stagnant steam atmosphere inside the perforated cladding was found to promote increased absorption of hydrogen in the cladding. Hydrogen concentrations of about 50 to 100 ppm were found to embrittle the zircaloy cladding. The F_W values in the range 0.8 to 0.9 reported by Homma et al. are

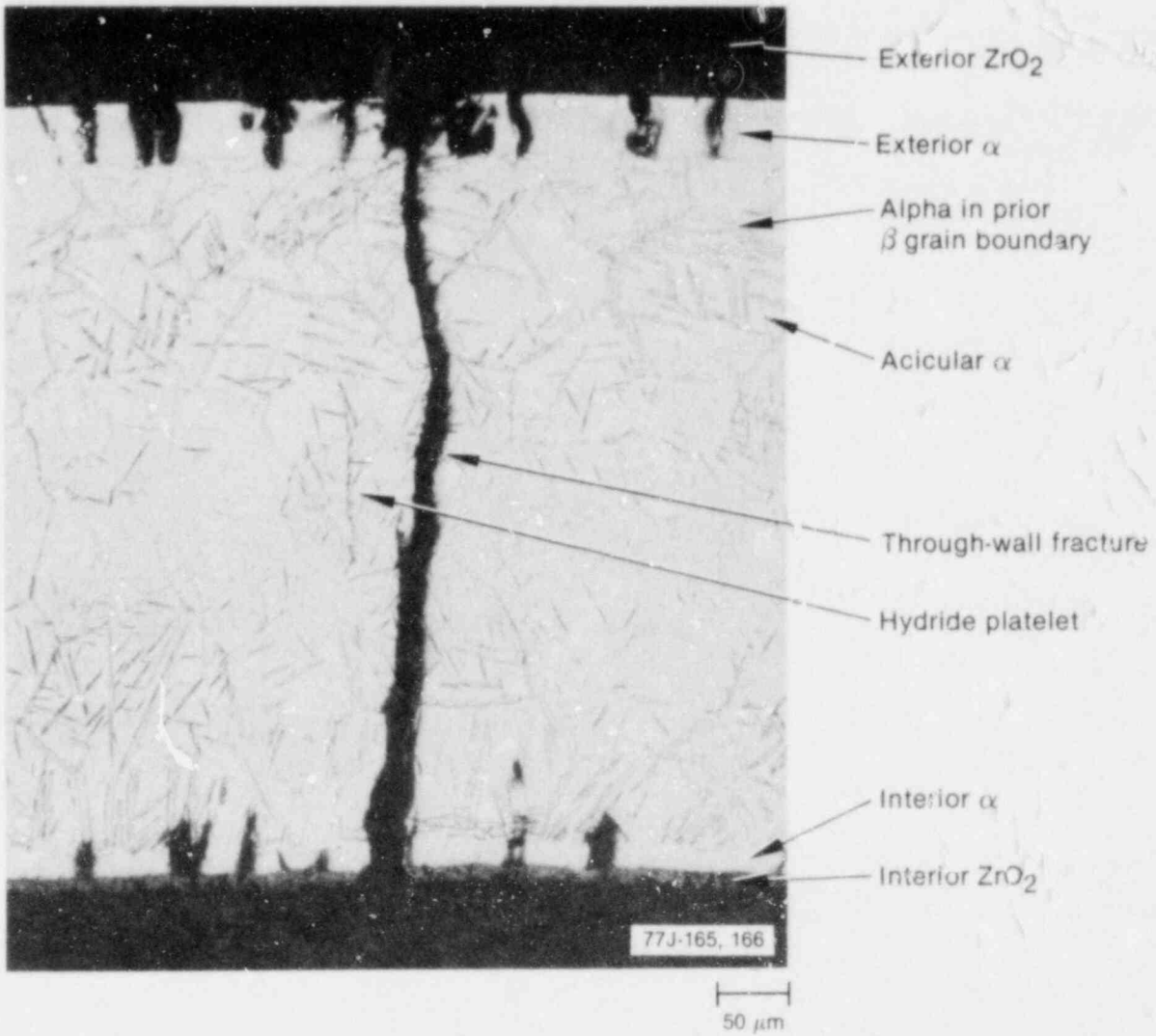

Figure 15. Microstructure in region of fracture at 0.571-m elevation of Rod IE-019.

in good agreement with the F_W values (0.73 to 0.88) measured at the fractures of Rods IE-019 and A-0021.

The hydrogen concentration (340 and 1020 ppm) adjacent to the fractures in Rods A-0021 and IE-019, respectively, was well in excess of the 50 to 100 ppm reported by Homma et al. to embrittle breached zircaloy cladding. However, several specimens listed in Table 1 were taken from rods that did not fracture but also had hydrogen concentrations of >100 ppm. With the exception of Rods A-0021 and IE-019, the rods in Table 1 exhibited limited development of alpha material in the prior beta grain boundaries.

A hydride platelet can be seen in Figure 15 adjacent and parallel to the through-wall fracture in Rod IE-019. Such long, radially oriented hydrides are detrimental to cladding ductility and could play a major role in the embrittlement of breached rods. Rim alpha and acicular alpha-phase material in the transformed beta phase, in conjunction with elevated hydrogen content, may be responsible for the anomalous embrittlement of the two PBF fuel rods (A-0021 and IE-019) that operated with breached cladding. More details on the effect of hydrogen on the oxygen embrittlement of beta-quenched zircaloy-4 cladding can be found in Reference 7. The microstructural, microhardness, and embrittlement characterizations of the hydrogen-affected regions suggest that the presence of hydrogen in the various beta-quenched phases may be an important factor in the consideration of the fracture resistance of zircaloy cladding under some oxidizing conditions.[7]

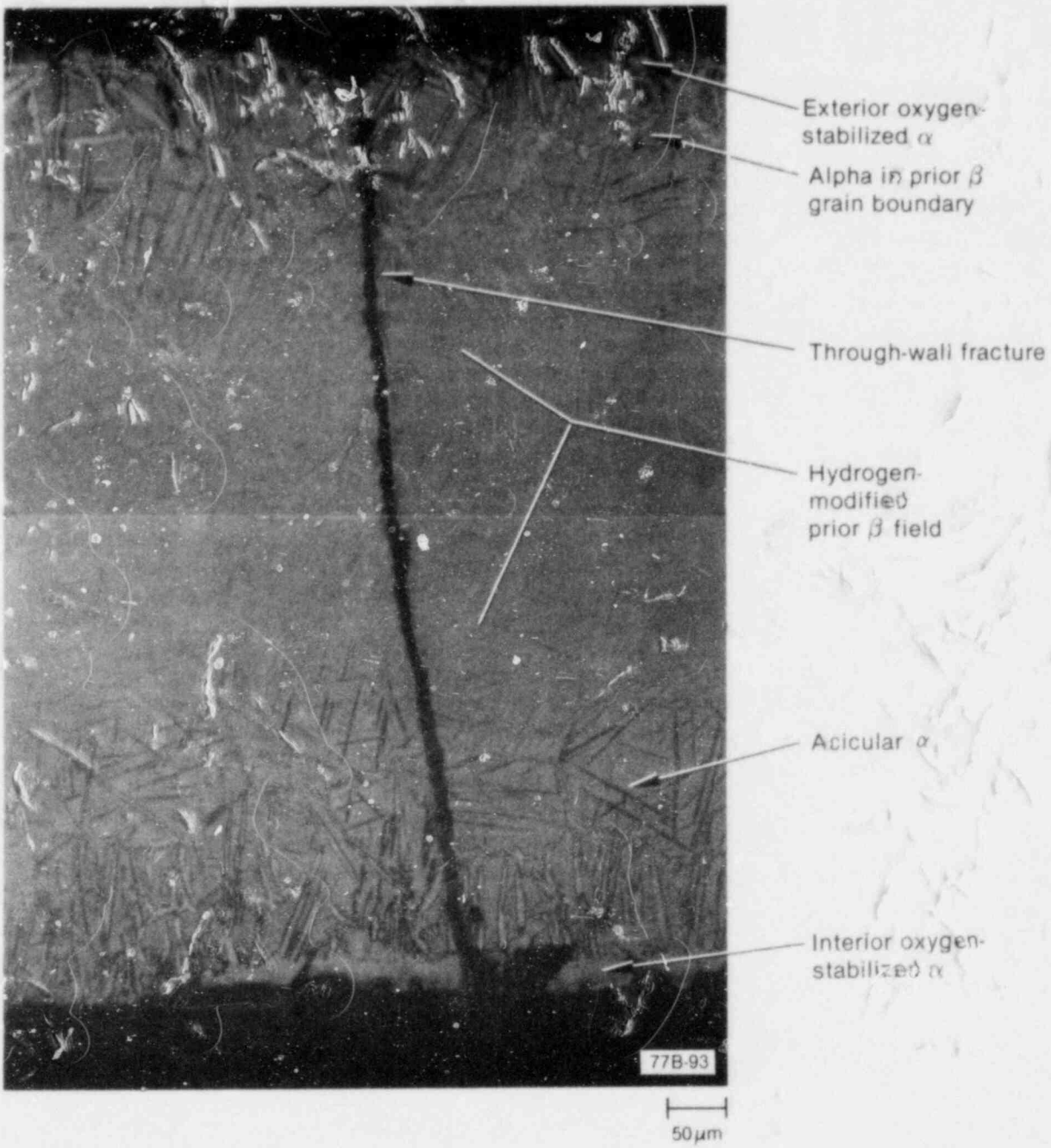

Figure 16. Microstructure in region of fracture at 0.425-m elevation of Rod A-0021.

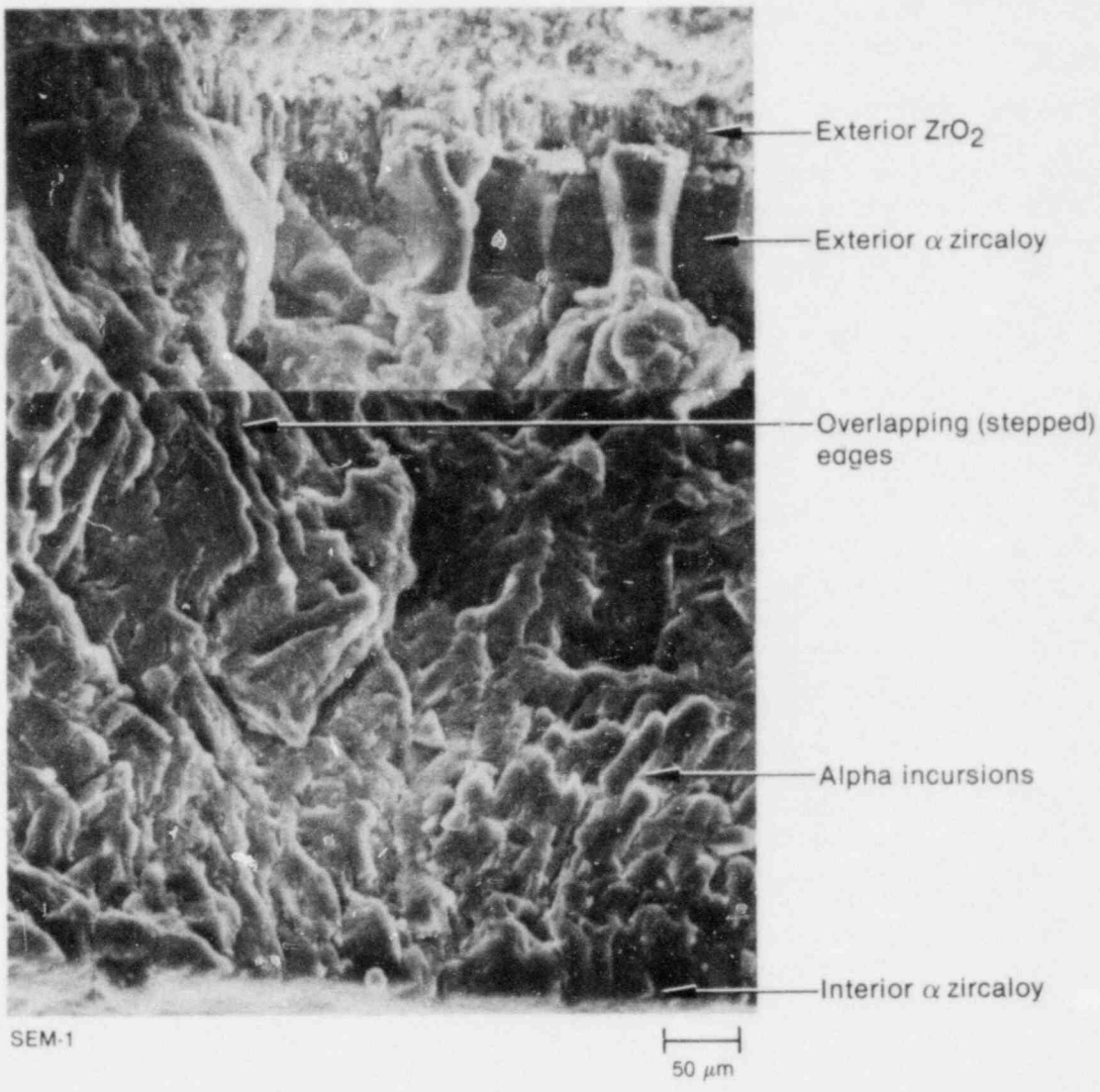

Figure 17. Scanning electron micrograph of the cross-wall fracture at 0.502-m elevation of Rod IE-019, exhibiting grain boundary alpha and hydrogen-modified microstructure.

4. CONCLUSIONS

Embrittlement criteria for zircaloy cladding were compared with fracture data from in-pile and out-of-pile tests. Analysis of the results led to the following observations and conclusions:

1. The fractional thickness of the remaining beta phase criterion, $F_W \leq 0.5$, and the equivalent cladding reacted criterion, ECR $\leq 17\%$, poorly predict zircaloy cladding thermal shock (quenching) failures and do not predict fuel handling failures.

2. Chung and Kassner's embrittlement criterion for thermal shock (thickness of the cladding with ≤ 0.9 wt% oxygen should be greater than 0.1 mm) fits the in-pile data.

3. Three PBF handling failures were not predictable by Chung and Kassner's criterion for handling failure (thickness of the cladding with ≤ 0.7 wt% oxygen should be greater than 0.3 mm). These failures were from two rods operated during film boiling testing with breached cladding, which exhibited a modified prior beta microstructure and enhanced hydrogen absorption (> 300 ppm H_2) due to stagnant steam within the test rods.

4. Pawel's criteria of 95% oxygen saturation of beta-zircaloy and 0.7 wt% oxygen in the beta-zircaloy accounted for all the thermal shock and most of the handling fractures in both the in-pile and out-of-pile experiments. The three PBF handling failures not predicted by the Pawel's embrittlement criteria are from the two test rods that operated with breached cladding during film boiling testing; they are the same three failures not predicted by Chung and Kassner's criterion for handling failure.

5. PBF rods that operated with breached cladding during film boiling testing were embrittled to a greater extent than intact rods oxidized under similar conditions. The handling fractures of those rods were not predicted by any of the embrittlement criteria.

6. The failure boundary (based on time-at-oxidation temperature for thermal shock) for out-of-pile data is more conservative than that drawn for the limited number of in-pile quenching failures.

7. Pawel's embrittlement criteria could be used for predicting rod failures in the PBF SFD tests but would not specify the cause of failure (quenching or handling). Chung and Kassner's embrittlement criteria for thermal shock and handling failures are recommended for evaluating and predicting the PBF SFD tests in particular and severe fuel damage accidents in general.

REFERENCES

1. J. M. Broughton, *Severe Core Damage Assessment Program Experiment Requirements*, EGG-TFBP-5067, March 1980.

2. H. M. Chung and T. F. Kassner, *Embrittlement Criteria For Zircaloy Fuel Cladding Applicable to Accident Situations in Light-Water Reactors*, NUREG/CR-1344, ANL-79-48, January 1980.

3. U.S. Nuclear Regulatory Commission, Office of Nuclear Regulatory Research, *A Description of the Current and Planned Reactor Safety Research Sponsored by the Nuclear Regulatory Commission's Division of Reactor Safety Research*, Report NUREG-75/058, June 1975.

4. S. L. Seiffert and R. R. Hobbins, *Oxidation and Embrittlement of Zircaloy-4 Cladding from High-Temperature Film Boiling Operation*, NUREG/CR-0517, TREE-1327, April 1979.

5. N. L. Hampton and D. L. Hagrman, *Cladding Oxidation (CORROS, COBILD, COXIDE, COXWTK and COXTHK)*, EGG-CDD-5647, November 1981.

6. R. R. Hobbins et al., "Embrittlement of Zircaloy-Clad Fuel Rods Irradiated Under Film Boiling Conditions," *Zirconium in the Nuclear Industry (Fourth Conference), ASTM STP 681, American Society for Testing and Materials*, 1979, pp. 586-599.

7. S. L. Seiffert, *The Effect of Hydrogen on the Oxygen Embrittlement of Beta Quenched Zircaloy-4 Fuel Cladding*, Zirconium in the Nuclear Industry (Fifth Conference), ASTM STP 754, American Society for Testing and Materials, January 1982, pp. 303-327.

8. T. G. Odekirk, *Detailed Test Plan Report for PBF Test Series PCM-20: The Behavior of Unirradiated PWR Fuel Rods Under Power-Cooling-Mismatch Conditions*, ANCR-1095 April 1974.

9. P. E. MacDonald et al., "Response of Unirradiated and Irradiated PWR Fuel Rods Tested Under Power-Cooling-Mismatch Conditions," *Nuclear Safety, 19* (4), 1978.

10. G. W. Cawood et al., *Power-Cooling-Mismatch Test Series, Test PCM-2A Test Results Report*, ANCR-1347, September 1976.

11. S. L. Seiffert and G. R. Smolik, *Postirradiation Examination Results for the Power-Cooling-Mismatch Test 2A*, TREE-NUREG-1029, February 1977.

12. Z. R. Martinson et al., *Power-Cooling-Mismatch Test Series, Test PCM-2 Test Results Report*, TREE-NUREG-1038, February 1977.

13. S. L. Seiffert, *Power-Cooling-Mismatch Test Series, Test PCM-2 Postirradiation Examination*, TREE-NUREG-1069, March 1977.

14. S. L. Seiffert, *Power-Cooling-Mismatch Test Series, Test PCM-4 Postirradiation Examination*, TREE-NUREG-1187, December 1977.

15. S. L. Seiffert and T. F. Cook, *Power-Cooling-Mismatch Test Series, Test PCM-4 Postirradiation Examination*, TREE-NUREG-1230, July 1978.

16. W. J. Quapp et al., *Irradiation Effects Test Series, Scoping Test 1 Test Results Report*, TREE-NUREG-1066, September 1977.

17. A. S. Mehner et al., *Postirradiation Examination Results for the Irradiation Effects Scoping Test 1*, ANCR-NUREG-1335, September 1976.

18. W. J. Quapp et al., *Irradiation Effects Test Series, Scoping Test 2 Test Results Report*, TREE-NUREG-1044, September 1977.

19. A. S. Mehner, *Postirradiation Examination Results for the Irradiation Effects Scoping Test 2*, TREE-NUREG-1022, January 1977.

20. W. J. Quapp et al., *Irradiation Effects Test Series, Test IE-1 Test Results Report*, TREE-NUREG-1046, March 1977.

21. A. S. Mehner and R. S. Semken, *Postirradiation Examination Results for the Irradiation Effects Test IE-1*, TREE-NUREG-1199, February 1978.

22. C. M. Allison et al., *Irradiation Effects Test Series, Test IE-2 Test Results Report*, TREE-NUREG-1074, August 1977.

23. S. A. Ploger et al., *Postirradiation Examination Results for the Irradiation Effects Test 2*, TREE-NUREG-1195, January 1978.

24. L. C. Farrar et al., *Irradiation Effects Test Series, Test IE-3 Test Results Report*, TREE-NUREG-1106, October 1977.

25. S. A. Ploger and T. F. Cook, *Postirradiation Examination Results for the Irradiation Effects Test IE-3*, TREE-NUREG-1220, March 1978.

26. D. W. Croucher et al., *Irradiation Effects Test Series, Test IE-5 Test Results Report*, TREE-NUREG-1130, January 1978.

27. T. G. Cook et al., *Postirradiation Examination Results for the Irradiation Effects Test IE-5*, TREE-NUREG-1201, March 1978.

28. B. A. Cook, *Fuel Rod Material Behavior During Test PCM-1*, NUREG/CR-0757, TREE-1333, June 1979.

29. D. K. Kerwin, *Test PCM-5 Fuel Rod Materials Behavior*, NUREG/CR-1430, EGG-2033, May 1980.

30. R. E. Mason of EG&G Idaho, Inc., Personal Communication Regarding PCM-7 Test Results, April 1982.

31. R. E. Pawel et al., "Diffusion of Oxygen in Beta-Zircaloy and the High Temperature Zircaloy-Steam Reaction," *Zirconium in the Nuclear Industry*, ASTM STP 633, A. L. Lowe, Jr. and G. W. Parry (eds.), American Society for Testing and Materials, 1979, pp. 119-133.

32. R. R. Hobbins, G. R. Smolik, G. W. Gibson, "Zircaloy Cladding Behavior During Irradiation Tests Under Power-Cooling-Mismatch Conditions," *Zirconium in the Nuclear Industry*, ASTM STP 633, A. L. Lowe and G. W. Parry (eds.), American Society for Testing and Materials, 1977, pp. 182-208.

33. C. J. Scatena, *Fuel-Cladding Embrittlement During a Loss-of-Coolant Accident*, NEDO-10674, October 1972.

34. R. E. Pawel, "Oxidation Diffusion in Beta Zircaloy During Steam Oxidation," *Journal of Nuclear Materials, 50*, 1974, pp. 247-258.

35. D. W. Croucher, "Behavior of Defective Pressurized Water Reactor Fuel Rods During Power Ramp and Power-Cooling-Mismatch Conditions," *Nuclear Technology*, Volume 51, November 1980, pp. 45-57.

36. D. O. Hobson, "Ductile-Brittle Behavior of Zircaloy Fuel Cladding," *Proceedings of the Topical Meeting on Water Reactor Safety, Salt Lake City, Utah*, CONF-730304, March 1973, pp. 274-288.

37. K. Homma et al., *Behavior of Inner Surface Oxidation of the Zircaloy Cladding Tube in a Loss-of-Coolant Accident*, JAERI-M-6602, June 1976.

38. K. Homma, T. Furuta, S. Kawasaki, *Behavior of the Zircaloy Cladding Tube in a Mixed Gas of Hydrogen and Steam*, JAERI-7131, NUREG/TE-0021, June 1977.

APPENDIX A
OXIDATION HISTORIES OF THE PBF AND THE ANL TESTS

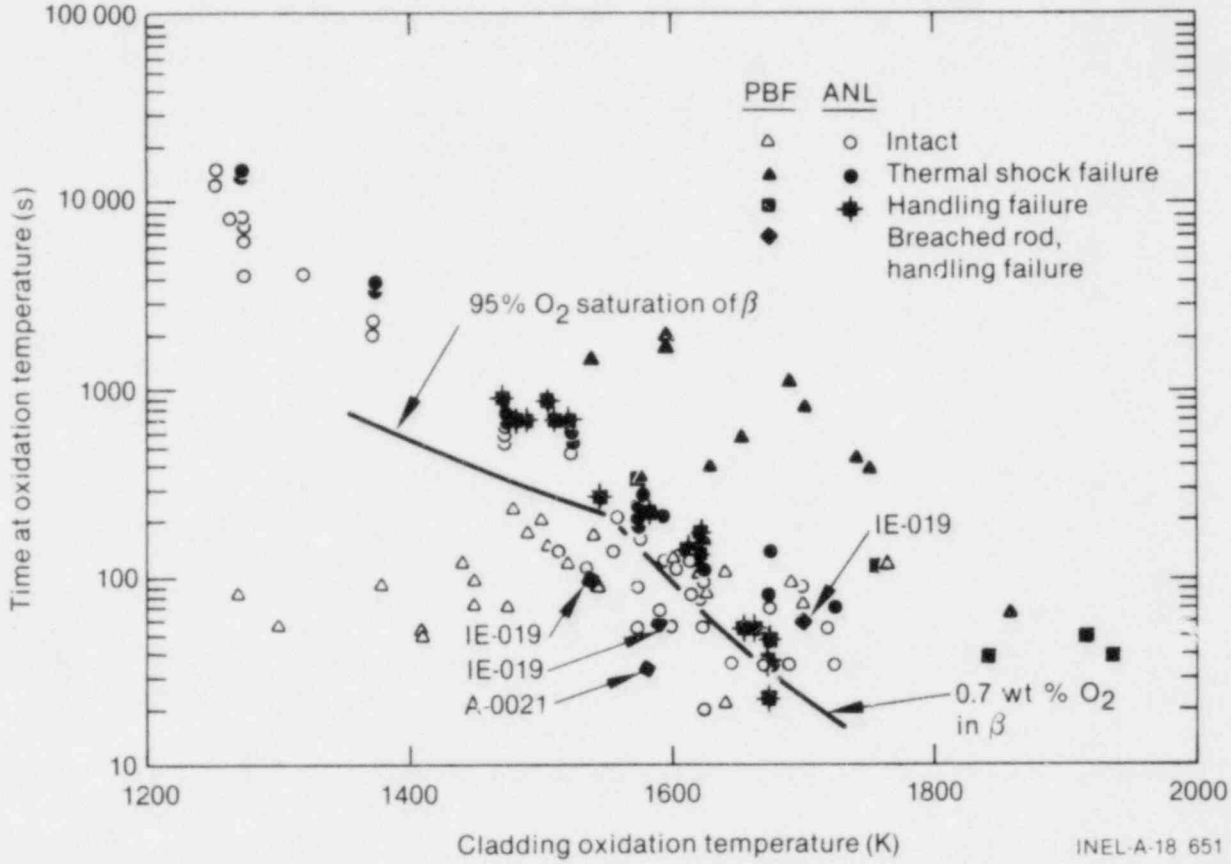

Figure A-1. Failure map for PBF and ANL experiments.

Table A-1. Oxidation histories of the PBF test rods (PCM and IE tests).

Rod	Elevation From Bottom of Fuel Stack (m)	Pretest Cladding Wall Thickness (mm)	Exposure Time In Film Boiling (s)	Isothermal Effective Cladding Temperature (K)	Adjusted Time in Film Boiling[a] (s)	Rod Failure
UTA-0004	0.581[b]	0.61	345	1740	436	Rod failed in-pile 60 s after shutdown
UTA-0004	0.505[b]	0.61	260	1575	329	Rod failed in-pile and fractured during posttest handling
UTA-0005	0.567	0.61	39	1410	49	Intact rod
UTA-0006	0.768	0.61	78	1450	99	Intact rod
UTA-0007	0.663	0.61	180	1480	228	Intact rod
UTA-0008	0.533	0.61	101	1600	128	Intact rod
A-0014	0.623	0.61	57	1450	72	Intact rod
A-0015	0.483	0.61	17	1640	22	Intact rod
A-0021	0.425[b]	0.61	26	1580	33	In-reactor breach, and fracture during posttest handling
UTA-0014	0.600	0.61	55	1475	70	Intact rod
UTA-0015	0.606	0.61	67	1625	85	Intact rod
UTA-0016	0.667	0.61	136	1490	172	Intact rod
UTA-0017	0.629	0.61	116	1505	147	Intact rod

Table A-1. (continued)

Rod	Elevation From Bottom of Fuel Stack (m)	Pretest Cladding Wall Thickness (mm)	Exposure Time In Film Boiling (s)	Isothermal Effective Cladding Temperature (K)	Adjusted Time in Film Boiling[a] (s)	Rod Failure
1E-001	0.482	0.59	70	1690	95	Intact rod
1E-001	0.597[b]	0.59	288	1630	389	Rod failed in-pile 80 s after shutdown
1E-005	0.794	0.59	37	1410	50	Intact rod
1E-007	0.501[b]	0.59	48	1860	65	Rod failed in-pile 180 s after shutdown
1E-008	0.559	0.59	20	1540	27	Rod breached in-pile due to massive hydriding[c]
1E-009	0.565	0.59	60	1270	81	Intact rod
1E-010	0.559	0.59	79	1640	107	Intact rod
1E-011	0.592	0.62	94	1760	115	Intact rod
1E-012	0.580	0.62	75	1380	92	Intact rod
1E-013	0.592	0.59	87	1520	118	Intact rod
1E-014	0.598	0.59	91	1440	123	Intact rod
1E-015	0.584[b]	0.59	84	1750	114	Rod failed during posttest handling

Table A-1. (continued)

Rod	Elevation From Bottom of Fuel Stack (m)	Pretest Cladding Wall Thickness (mm)	Exposure Time In Film Boiling (s)	Isothermal Effective Cladding Temperature (K)	Adjusted Time in Film Boiling[a] (s)	Rod Failure
IE-016	0.539[b]	0.59	36	1920	49	Rod failed during posttest handling
IE-017	0.578	0.59	71	1540	96	Intact rod
IE-018	0.595	0.59	78	1620	105	Intact rod
IE-019	0.502[b]	0.60	44	1700	58	In-reactor breach, and fracture during posttest handling
IE-019	0.571[b]	0.60	44	1590	58	In-reactor breach, and fracture during posttest handling
IE-019	0.625[b]	0.60	76	1535	99	In-reactor breach, and failure during posttest handling
IE-020	0.568	0.60	56	1700	73	Intact rod
IE-021	0.527[b]	0.61	31	1840	39	Rod failed in-pile 90 s after shutdown, and handling fracture
IE-022	0.495[b]	0.61	31	1940	39	Rod failed in-pile 90 s after shutdown, and handling fracture
201-1	0.670	0.61	895	1690	1132	In-pile breach and failure during film boiling
205-1	0.580	0.62	665	1700	814	Rod failed in-pile at ∿500 s in film boiling

Table A-1. (continued)

Rod	Elevation From Bottom of Fuel Stack (m)	Pretest Cladding Wall Thickness (mm)	Exposure Time In Film Boiling (s)	Isothermal Effective Cladding Temperature (K)	Adjusted Time in Film Boiling[a] (s)	Rod Failure
205-3	0.680	0.62	165	1500	202	Intact rod
205-4	0.680	0.62	--	1850	--	Rod failed during posttest handling
205-5	0.680	0.62	135	1540	165	Intact rod
205-6	0.780	0.62	45	1300	55	Intact rod
205-8	0.68	0.62	310	1750	380	Rod failed in-pile at 250 s in film boiling
207-1	0.622	0.61	250	1570	316	Intact rod
207-2	0.533[b]	0.61	1600	>1600	2024	Rod failed in-pile
207-3	0.622[b]	0.61	440	>1650	556	Rod failed in-pile
207-4	0.680[b]	0.61	440	>1600	1771	Rod failed in-pile
207-6	0.554	0.61	1160	>1540	1467	Rod failed in-pile

a. Adjusted time correction factor is (0.686 mm/original cladding wall thickness)^2.

b. Fracture location.

c. Failure not attributed to PCM conditions.

Table A-2. Oxidation histories of the ANL zircaloy-4 cladding[a] cooled through the $\beta \rightarrow \alpha'$ phase transformation at ~100 K/s

Test Number	Maximum Isothermal Oxidation Temperature (K)	Time at the Isothermal Oxidation Temperature (s)	Adjusted Time at the Isothermal Oxidation Temperature (s)	CIC[b]
421	1253	10 800	12 604	11
344	1253	12 780	14 915	11
30	1263	7 200	8 403	11
294	1273	13 020	15 195	72
311	1273	3 600	4 201	11
321	1273	5 400	5 400	11
335	1273	11 880	13 865	11
384	1273	6 900	8 053	11
392	1273	7 200	8 403	11
401	1273	12 000	14 005	11
365	1273	12 480	14 565	11
375	1318	3 600	4 201	11
1662	1373	1 997	2 331	11
1669	1373	1 997	2 331	11
1686	1373	3 000	3 501	73
1692	1373	3 300	3 851	73
1701	1373	1 697	1 981	11
1479	1473	600	700	73
1489	1473	503	587	11
1499	1473	551	643	73
1509	1473	450	525	11
1519	1473	647	755	74
1845	1513	120	140	11
1522	1523	401	468	11
1539	1523	450	525	95
1549	1523	503	587	95
1563	1533	95	111	11
1842	1553	120	140	11
1413	1558	180	210	11
1429	1573	210	245	95
1459	1573	167	195	11
1463	1573	150	175	11
1466	1573	150	175	11
1439	1573	180	210	95
1745	1573	47	55	11
1736	1573	77	90	11
1409	1578	240	280	73
1786	1588	60	70	11
1449	1593	180	210	94
1622	1593	107	125	11
1743	1598	47	55	11
1564	1603	95	111	11
1623	1613	107	125	11
1612	1613	71	83	11
1644	1623	83	97	11

Table A-2. (continued

Test Number	Maximum Isothermal Oxidation Temperature (K)	Time at the Isothermal Oxidation Temperature (s)	Adjusted Time at the Isothermal Oxidation Temperature (s)	CIC[b]
5810	1623	95	111	94
5899	1623	95	111	94
5897	1623	95	111	11
5898	1623	95	111	11
5813	1623	95	111	94
1592	1623	17	20	11
1608	1623	131	153	93
1609	1623	131	153	94
1611	1623	71	83	11
1744	1623	47	55	11
1727	1643	30	35	11
1722	1668	30	35	11
1765	1673	60	70	11
1844	1673	120	140	95
1851	1673	71	83	95
1725	1673	30	35	11
1714	1688	30	35	11
1737	1698	77	90	11
1742	1718	47	55	11
1723	1723	30	35	11
1762	1723	60	70	95

a. The original cladding wall thickness is 0.635 mm.

b. CIC = cladding integrity code = 11 denotes cladding intact after thermal shock; 7X and 9X denote thermal-shock failure in a nonballooned or ballooned region on the tube, respectively, where X signifies the number of cladding fragments; X = 5 denotes ≥ 5.

APPENDIX B
LISTING OF THE COBILD SUBCODE AND ITS DRIVER

```
CCCCCCCCCCCCCCCCCCCCCCCCCCCCCCCCCCCCCCCCCCCCCCCCCCCCCCCCCCCCCCCCCC
      SUBROUTINE COBILD ( TI, TF, DT,AF5, DROD, PINT,IP2, Y8 , Y9,
CCCCCCCCCCCCCCCCCCCCCCCCCCCCCCCCCCCCCCCCCCCCCCCCCCCCCCCCCCCCCCCCCCC
     *                     Y9A,Y9B,AA0,AB0,AC0,AD0,AE0,AF0,AG0,AH0,AI0,
     *                     AAI,ABI,ACI,ADI,AEI,AFI,AGI,AHI,AII, W1,  P,
     *                     PERSAT , BWTFR ,ALB , KRAP )
C
C
C     THIS PROGRAM WAS ADAPTED FROM THE PROGRAM "BUILD5" WRITTEN BY
C     R.E. PAWEL OF OAK RIDGE NATIONAL LABORATORY (ORNL).
C
C     DATA AND ANALYSES FROM J.V. CATHCART OF ORNL ARE USED TO COMPUTE
C     THE ZRO2 AND OXYGEN-STABILIZED ALPHA THICKNESSES ON THE CLADDING
C     OUTER SURFACE AND SIMILAR EQUATIONS FROM P. HOFMANN OF THE
C     KERNFORSCHUNGSZENTRUM KARLSRUHE (KFK) FOR OXYGEN-STABILIZED
C     ALPHA LAYERS ON THE CLADDING INNER SURFACE WHEN THERE IS FUEL
C     PELLET-CLADDING MECHANICAL INTERACTION (PCMI).
C
C     OXYGEN PROFILES ARE COMPUTED ON THE BASIS OF A
C     FINITE DIFFERENCE METHOD ASSUMING THE TRANSIENT TO BE COMPOSED
C     OF A SERIES OF ISOTHERMAL SEGMENTS.
C
C
C     P        = OUTPUT LINEAR POWER GENERATED BY THE ZR+O2 = ZRO2
C                  REACTION(W/M).
C     PERSAT   = OUTPUT PER CENT SATURATION OF THE BETA (UNITLESS).
C     BWTFR    = OUTPUT AVERAGE OXYGEN CONCENTRATION IN BETA
C                  (WEIGHT FRACTION).
C     ALB      = OUTPUT BETA THICKNESS (M).
C
C     IP2      = OUTPUT/INPUT PCMI PARAMETER
C                 IP2 = 0 IMPLIES NO PCMI--LAST STEP WHEN INPUT
C                         THIS STEP WHEN OUTPUT.
C                 IP2 = 2 IMPLIES PCMI--LAST STEP WHEN INPUT
C                         THIS STEP WHEN OUTPUT.
C     Y8       = OUTPUT/INPUT OXIDE THICKNESS(M).
C     Y9       = OUTPUT/INPUT THICKNESS OF OXYGEN-STABILIZED ALPHA
C                  NEAREST TO THE OUTER CLADDING SURFACE (M).
C     Y9A      = OUTPUT/INPUT THICKNESS OF OXYGEN-STABILIZED ALPHA
C                  NEAREST TO THE UO2 FUEL (M).
C     Y9B      = OUTPUT/INPUT THICKNESS OF OXYGEN-STABILIZED ALPHA
C                  BETWEEN Y9 AND Y9A (M).
C     AA0 TO
C       AI0    = OUTPUT/INPUT OXYGEN CONCENTRATIONS AT EQUIDISTANT NODES
C                IN THE BETA
C                 AA0 = CONCENTRATION AT THE ALPHA-BETA INTERFACE AND
C                 AI0 = CONCENTRATION AT THE INNER BETA SURFACE IF
C                         THERE IS NO PCMI OR AT THE BETA MIDPOINT IF
C                         THERE IS PCMI.
C     AAI TO
C       AII    = OUTPUT/INPUT OXYGEN CONCENTRATIONS AT EQUIDISTANT NODES
C                IN THE INNER HALF OF THE BETA IF THERE IS PCMI.
C                 AAI = THE CONCENTRATION AT THE INNER ALPHA-BETA
C                         INTERFACE AND
C                 AII = THE CONCENTRATION AT THE BETA MIDPOINT.
C                  ALL CONCENTRATIONS ARE IN WEIGHT FRACTION OF OXYGEN.
C     W1       = OUTPUT/INPUT OXYGEN UPTAKE THROUGH THE OUTER CLADDING
C                  SURFACE (KG/M**2).
C     KRAP     = OUTPUT/INPUT EROR FLAG
C                 KRAP = 0 IF NO ERRORS DETECTED
C                 KRAP = 1 IF CORRELATION RANGE EXCEEDED
C                 KRAP = 2 IF IMPOSSIBLE INPUT DETECTED
C     TI       = INPUT CLADDING TEMPERATURE AT START OF TIME STEP(K).
C     TF       = INPUT CLADDING TEMPERATURE AT END OF TIME STEP (K).
C     DT       = INPUT DURATION OF TIME STEP (S).
C     AF5      = INPUT WALL THICKNESS OF AS-FABRICATED ROD (M).
C     DROD     = INPUT DIAMETER  OF AS-FABRICATED ROD (M).
C     PINT     = INPUT PELLET-CLADDING INTERFACE PRESSURE (PA).
C
C    THE EQUATIONS USED IN THIS SUBROUTINE ARE BASED ON DATA FROM
C    (1) J. V. CATHCART. QUARTRLY PROGRESS REPORT ON THE ZIRCONIUM
C        METAL-WATER OXIDATION KINETICS PROGRAM SPONSORED BY THE NRC
```

```
C          DIVISION OF REACTOR SAFETY RESEARCH FOR OCTOBER-DECEMBER
C          1976, ORNL/NUREG/TM-67 (FEBRUARY 1977).
C     (2)  W. K. JOHNSON AND T. R. MCELRACK, "HIGH TEMPERATURE OXIDATION
C          OF ZIRCALOY-2 AND ZIRCALOY-4 IN STEAM," JOURNAL OF NUCLEAR
C          MATERIALS 75 (1978), PP. 201-201.
C     (3)  P. HOFMANN, G. KOLITSCH, "CHEMICAL INTERACTION BETWEEN UO2
C          AND ZRY-4 IN THE TEMPERATURE RANGE BETWEEN 900 AND 1500 C,"
C          PAPER PRESENTED AT THE FOURTH INTERNATIONAL CONFERENCE ON
C          ZIRCONIUM IN THE NUCLEAR INDUSTRY, STRATFORD-UPON-AVON,
C          ENGLAND, JUNE 26-29, 1979.
C     (4)  L. BAKER AND L. C. JUST, STUDIES OF METAL-WATER REACTIONS
C          AT HIGH TEMPERATURES-III. EXPERIMENTAL AND THEORETICAL
C          STUDIES OF THE ZIRCONIUM-WATER REACTION, ANL-6548 (MAY 1962)
C     (5)  R. E. PAWEL, "DIFFUSION IN A FINITE SYSTEM WITH A MOVING
C          BOUNDARY," JOURNAL OF NUCLEAR MATERIALS, 49 (JANUARY 1974)
C          PP. 281-290.
C     (6)  R. A. PERKINS, ZIRCONIUM METAL WATER OXIDATION KINETICS II,
C          OXYGEN-18 DIFFUSION IN A ZIRCALOY, ORNL/NUREG/TM-19(1976).
C     (7)  R. E. PAWEL, R. A. PERKINS, R. A. MOREL, J. V. CATHCART,
C          G. J. YUREK, AND F. C. ORDSCHEL, "DIFFUSION OF OXYGEN IN
C          BETA-ZIRCALOY AND THE HIGH TEMPERATURE ZIRCALOY-STEAM
C          REACTION," ZIRCONIUM IN THE NUCLEAR INDUSTRY, ASTM STP 663
C          (1977) PP. 119-133.
C
C     THIS MODEL SHOULD NOT BE USED OUTSIDE THE TEMPERATURE RANGE 1273-
C     2100K OR FOR PROBLEMS WHICH CAUSE THE BETA PHASE REGION TO BECOME
C     MUCH SMALLER THAN THE REMAINDER OF THE CLADDING
C
C      RECOMMENDED INPUT VALUES FOR A FRESH FLD ARE:
C           PINT = 0.0
C           AA0 TO A10, ALL = 0.0012
C           AA1 TO A11, ALL = 0.0
C           Y8,Y9,Y9A,Y9B, AND W1, ALL = 0.0
C           IP2 = 0
C
C      CCBILD WAS CODED BY G.A. REYMANN IN JULY 1977.
C      UPDATED BY G.A. REYMANN IN APRIL 1979.
C      UPDATED BY G. M. BEERS TO IMPROVE PROGRAM EFFICIENCY
C           AND ADD INPUT CHECK IN NOVEMBER 1981 (CCLF-MP-07)
C
C
      DIMENSION AA(6),AB(6),AC(6),AD(6),AE(6),AF(6),AG(6),AH(6),AI(6)
C
C
C  SAVE INCOMING VALUE OF THE KRAP ERROR FLAG
C
      IKRAP  = KRAP
C
C  TEST INPUT FOR PROPER RANGES.  SET KRAP ERROR FLAG TO SPECIFIED VALUES
C  IF EXCEPTIONS ARE FOUND.
C
      IF  (     DT  .LE.  0.0
     +     .OR.  AM5  .LE.  0.0
     +      .OR.  DROD  .LE.  0.0
     +       .OR.  Y8    .LT.  0.0
     +        .OR.  Y9    .LT.  0.0
     +         .OR.  Y9A   .LT.  0.0
     +          .OR.  Y9B   .LT.  0.0
     +           .OR.  W1    .LT.  0.0  )  THEN
C
C  SET KRAP ERROR FLAG TO 2 AND CHECK INCOMING KRAP VALUE FOR CHANGE
C
C
C
          KRAP  = 2
C
          IF  ( IKRAP .NE. 2 )  THEN
C
              WRITE  ( 6 , 901 )
              WRITE  ( 6 , 902 )  DT , AM5 , DROD , Y8 , Y9 , Y9A ,
     +                            Y9B , W1
```

```
C           ENDIF
C
C           RETURN
C
C       ENDIF
C
C
        IF  (     AAD  .LT.  0.00119
     +       .OR.  ABD  .LT.  0.00119
     +       .OR.  ACD  .LT.  0.00119
     +       .OR.  ADD  .LT.  0.00119
     +       .OR.  AED  .LT.  0.00119
     +       .OR.  AFD  .LT.  0.00119
     +       .OR.  AGD  .LT.  0.00119
     +       .OR.  AHD  .LT.  0.00119
     +       .OR.  AID  .LT.  0.00119 )  THEN
C
C SET KRAP ERROR FLAG TO 2 AND CHECK INCOMING KRAP VALUE FOR CHANGE
C
            KRAP  = 2
C
            IF  ( IKRAP .NE. 2 )  THEN
C
                WRITE  ( 6 , 901 )
                WRITE  ( 6 , 903 )  AAD , ABD , ACD , ADD , AED ,
     +                              AFD , AGD , AHD , AID
                WRITE  ( 6 , 904 )  AAI , ABI , ACI , ADI , AEI ,
     +                              AFI , AGI , AHI , AII
C
            ENDIF
C
            RETURN
C
        ENDIF
C
C SAVE INPUT TEMPERATURES IN VARIABLES WHICH MAY BE ALTERED IF NECESSARY
C
        T1  =  TI
        T2  =  TF
        TS  =  DT
C
        IF  ( T1 .GT. 2100.0  .OR.  TF .GT. 2100.0 )  THEN
C
            IF(IKRAP .LT. 2) KRAP = 1
C
        ELSE  IF  ( T1 .LT. 1273.0  .OR.  TF .LT. 1273.0 )  THEN
C
            IF(IKRAP .LT. 2) KRAP = 1
C
            IF  ( T1 .LE. 1239.0  .AND.  TF .LE. 1239.0 )  THEN
C
               RETURN
C
            ELSE
                IF  ( TF .LT. 1239.0 )  THEN
C
                    T2  =  1239.0
                    TS  =  DT * ( TI - 1239.0 ) / ( T1 - TF )
C
C IF T1 IS < 1239 K THEN T2 IS SET TO 1239 AND A NEW TIME STEP TS IS
C CREATED JUST FOR USE WITHIN CUBO.LD.
                ELSE  IF  ( TI .LT. 1239.0 )  THEN
C
                    T1  =  1239.0
                    TS  =  DT * ( TF - 1239.0 ) / ( TF - T1 )
C
                ENDIF
C
```

```
         ENDIF
C
      ENDIF
C
C INITIALIZE THESE HOLDING VARIABLES
C
      AC20  =  0.0
      ACE0  =  0.0
C
      IPINT  =  INT( PINT )
C
C IPINT IS INTEGRAL PART OF PELLET-CLADDING INTERFACE PRESSURE
C
      IF  ( IPINT .NE. 0 )    THEN
C
          AM5  =  0.5 * AM5
C
      ENDIF
C
C SAVE INCOMING OXYGEN UPTAKE THROUGH OUTER CLADDING SURFACE IN W11
C
      W11  =  W1
C
C SET INTEGRATION TIME INCREMENT
C
      AZ3  =  TS * 0.2
C
      AK   =  ( T2 - T1 ) / TS
C
C CALCULATE TEMPERATURE DURING INTERVAL  (K)
C
      AZ6  =  ( T1 + T2 ) * .5
C
C CALCULATE BETA SATURATION CONCENTRATION
C
      IF  (  AZ6 .LT. 1373.0 )    THEN
C
          AS1  =  -0.0042607 + SQRT( ( AZ6 / 392.46 ) - 3.1417 )
C
      ELSE
C
          AS1  =  ( AZ6 - 1081.7 ) / 491.157
C
      ENDIF
C
      AS1  =  AS1 / 100.0
C
C
C CALCULATE D (OX IN BETA),  (CM2/S)
C
      AL5  =  2.6308-06 * EXP( -2.82E+04 / ( 1.987 * AZ6 ))
C
C
      IF  ( IPINT .NE. 0   .AND.   IP2 .EQ. 0 )  THEN
C
          IP2   =   2
          AAI   =   AI0
          ABI   =   ( AH0 + AI0 ) * 0.5
          ACI   =   AH0
          ADI   =   ( AG0 + AH0 ) * 0.5
          AEI   =   AG0
          AFI   =   ( AF0 + AG0 ) * 0.5
          AGI   =   AF0
          AHI   =   ( AE0 + AF0 ) * 0.5
          AII   =   AE0
          AI0   =   AE0
          AH0   =   ( AD0 + AE0 ) * 0.5
          AG0   =   AD0
```

```
            AFO    =  ( ACO + ADO ) * 0.5
            AGO    =  ACO
            AHO    =  ( ADO + AEO ) * 0.5
            AIO    =  AEO
            AAO    =  ( 3.0 * AAI + 6.0 * ABI - ACI ) * 0.125
C
      ELSE  IF  ( IPINT .EQ. 0   .AND.   IP2 .NE. 0 )  THEN
C
            IP2    =  0
            ABO    =  ACO
            ACO    =  AEO
            ADO    =  AGO
            AEO    =  ( AIO + AII ) * 0.5
            AFO    =  AGI
            AGO    =  AEI
            AHO    =  ACI
            AIO    =  AAI
            AAI    =  0.
            ABI    =  0.
            ACI    =  0.
            ADI    =  0.
            AEI    =  0.
            AFI    =  0.
            AGI    =  0.
            AHI    =  0.
            AII    =  0.
C
      ENDIF
C
      IP     =  0
      AA( 1 )   =  AAO
      AB( 1 )   =  ABO
      AC( 1 )   =  ACO
      AD( 1 )   =  ADO
      AE( 1 )   =  AEO
      AF( 1 )   =  AFO
      AG( 1 )   =  AGO
      AH( 1 )   =  AHO
      AI( 1 )   =  AIO
      GO  TO  225
C
  200 AA( 1 )   =  AAI
      AB( 1 )   =  ABI
      AC( 1 )   =  ACI
      AD( 1 )   =  ADI
      AE( 1 )   =  AEI
      AF( 1 )   =  AFI
      AG( 1 )   =  AGI
      AH( 1 )   =  AHI
      AI( 1 )   =  AII
C
  225 FIP = FLOAT( IP )
      AL2 = AM5 - ( 1.0 - FIP ) * ( 2.0 * Y8 / 3.0 + Y9 )
     +                                    - FIP * ( Y9A + Y9B )
C
      IF  ( IP2 .EQ. 0 )   THEN
C
          AL2  =  AL2 - ( Y9A + Y9B )
C
      ENDIF
C
C AL2 IS THE BETA THICKNESS AT START OF EACH TIME STEP.
C
C
      Y5    =  AZ3
  550 AZ8   =  T1 + AR * ( Y5 - AZ3 * 0.5 )
C
C AZ8 IS THE AVERAGE TEMP. DURING INCREMENT
C
      IF  ( IP .EQ. 1 )   THEN
```

```
C
            Y7A    =  COXTMP ( AZ6 , 3 )
            Y7B    =  COXTMP ( AZ6 , 4 )
C
            Y9A    =  SQRT( Y9A ** 2 + Y7A * AZ3 )
            Y9B    =  SQRT( Y9B ** 2 + Y7B * AZ3 )
C
C       ELSE
C
            Y6     =  COXTMP ( AZ6 , 1 )
            Y7     =  COXTMP ( AZ6 , 2 )
C
            Y8     =  SQRT( Y6 ** 2 + Y6 * AZ3 )
C
C  Y6 IS THE OXIDE LAYER THICKNESS AFTER INCREMENT.
C
            Y9     =  SQRT( Y9 ** 2 + Y7 * AZ3 )
C
C  Y9 IS THE ALPHA LAYER THICKNESS AFTER INCREMENT
C
            W2     =  COXWTR ( AZ6 )
C
            W1     =  SQRT( W1 ** 2 + W2 * AZ3 )
C
C  W1 IS THE TOTAL OXYGEN CONCENTRATION AFTER INCREMENT
C
            W11    =  Y8 * ( 5.62 ) * 0.26
C
C  W11 IS THE MINIMUM OXYGEN IN (KG/M**2) NECESSARY TO FORM
C  OXIDE LAYER.
C
            IF  ( ( W1 - W11 ) .LE.  0.0 )   THEN
C
                W1  =  W11
C
            ENDIF
C
        ENDIF
C
C
        Y5   = Y5 + AZ3
C
        IF  ( Y5 .LE. TS )   THEN
C
            GO  TO  550
C
        ENDIF
        FIP    =  FLOAT( IP )
        AL8    =  AM5 - ( 1.0 - FIP ) * ( .66667 * Y8 + Y9 )
     +                                        - FIP * ( Y9A + Y9B )
C
        IF  ( IP2 .EQ. 0 )   THEN
C
            AL8    =  AL8 - ( Y9A + Y9B )
C
        ENDIF
C
        IF  ( IP .EQ. 0 )   THEN
C
            AL80   =  AL8
C
        ENDIF
C
C  AL8 IS THE BETA THICKNESS AT END OF EACH TIME STEP
C
        AL4    =  AL2 - AL8
C
C  AL4 IS DELTA BETA DURING STEP
C
        AL7    =  AL2 * 0.125
```

```
C
      IF  ( AL4 .GT. AL7 )   THEN
C
          IF(IKKAP .LT. 2) KKAP = 1
C
          WRITE  ( 6 , 2771 )
C
      ENDIF
C
      AM3    =  AL4 / ( 2.0 * AL2 )
      AM4    =  ( AL4 ** 2 ) / ( 2.0 * ( AL2 ** 2 ) )
      AL6    =  AL6 * 0.125
C
C AL6 AS H(X), THE DISTANCE INCREMENT FOR FD NETWORK.
C
      AM1    =  ( AL6 ** 2 ) / ( AL5 * A23 )
C
      IF  ( AM1 .LT. 2.0 )   THEN
C
          IF(IKKAP .LT. 2) KKAP = 1
C
          WRITE  ( 6 , 5020 )
C
      ENDIF
C
C
C IN STEPS 2260 TO 2320 THE INITIAL OXYGEN CONCENTRATIONS ARE
C CALCULATED BY PARABOLIC INTERPOLATION. THIS IS NECESSARY DUE TO
C THE DECREASE IN BETA THICKNESS AS THE OTHER LAYERS GROW.
C
      AA( 1 )  =  AA( 1 ) + 8.0 * AM3 * ( 4.0 * AB( 1 ) - 3.0 * AA( 1 )
     +              - AC( 1 ) ) + 64.0 * AM4 * ( AC( 1 ) + AA( 1 )
     +              - 2.0 * AB( 1 ))
C
      IF  ( AS1 .GT. AA( 1 ) )   THEN
C
          AA( 1 )  =  AS1
C
      ENDIF
C
C
      AB(1) = AB(1) + 7.*AM3*(4.*AC(1)-3.*AB(1)-AD(1)) +
     #          49.0*AM4*(AD(1)+AB(1)-2.*AC(1))
C
      AC(1) = AC(1) + 6.*AM3*(4.*AD(1)-3.*AC(1)-AE(1)) +
     #          36.0*AM4*(AE(1)+AC(1)-2.*AD(1))
C
      AD(1) = AD(1) + 5.*AM3*(4.*AE(1)-3.*AD(1)-AF(1)) +
     #          25.0*AM4*(AF(1)+AD(1)-2.*AE(1))
C
       AE(1) = AE(1) + 4.*AM3*(4.*AF(1)-3.*AE(1)-AG(1)) +
     #          16.0*AM4*(AG(1)+AE(1)-2.*AF(1))
C
      AF(1) = AF(1) + 3.*AM3*(4.*AG(1)-3.*AF(1)-AH(1)) +
     #          9.0*AM4*(AH(1)+AF(1)-2.*AG(1))
C
      AG(1) = AG(1) + 2.*AM3*(4.*AH(1)-3.*AG(1)-AI(1)) +
     #          4.0*AM4*(AI(1)+AG(1)-2.*AH(1))
C
      AH(1) = AH(1) + 1.*AM3*(4.*AI(1)-3.*AH(1)-AH(1)) +
     #          1.0*AM4*(AH(1)+AH(1)-2.*AI(1))
C
      DO  2535  J = 2 , 6
C
          AA( J )  =  AA( 1 )
          AB( J )  =  (AA(J-1) + (AM1-2.)*AB(J-1) + AC(J-1))/(AM1)
          AC( J )  =  (AB(J-1) + (AM1-2.)*AC(J-1) + AD(J-1))/(AM1)
          AD( J )  =  (AC(J-1) + (AM1-2.)*AD(J-1) + AE(J-1))/(AM1)
          AE( J )  =  (AD(J-1) + (AM1-2.)*AE(J-1) + AF(J-1))/(AM1)
          AF( J )  =  (AE(J-1) + (AM1-2.)*AF(J-1) + AG(J-1))/(AM1)
```

```
            AG( J )   =  (AF(J-1) + (AM1-2.)*AG(J-1) + AH(J-1))/(AM1)
            AH( J )   =  (AG(J-1) + (AM1-2.)*AH(J-1) + AI(J-1))/(AM1)
            AI( J )   =  ((AM1-2.)*AH(J-1)+2.*AM(J-1))/AM1
C
 2535 CONTINUE
C
C
C CALCULATE OXYGEN IN BETA LAYER
C
C
      AQ2    = ( 6490. * AL6 ) / 3.
      AQ2    =  AQ2 * (AA( 6 ) + AI( 6 )
     +              + 2.0 * ( AC( 6 ) + AG( 6 ))
     +                  + 4.0 * ( AB( 6 ) + AD( 6 ) + AF( 6 ) + AH( 6 )))
C
      IF  ( IP .EQ. 1 )   THEN
C
            AAI    =  AA( 6 )
            ABI    =  AB( 6 )
            ACI    =  AC( 6 )
            ADI    =  AD( 6 )
            AEI    =  AE( 6 )
            AFI    =  AF( 6 )
            AGI    =  AG( 6 )
            AHI    =  AH( 6 )
            AII    =  AI( 6 )
            AM5    =  2.0 * AM5
            AL6    =  AL6 + AL60
            AQ2    =  AQ2 + AQ20
C
      ELSE
C
C AQ2 IS THE OXYGEN IN THE BETA, KG/M**2, (BY SIMPSON'S RULE)
C
            AQ20   =  AQ2
            AA0    =  AA( 6 )
            AB0    =  AB( 6 )
            AC0    =  AC( 6 )
            AD0    =  AD( 6 )
            AE0    =  AE( 6 )
            AF0    =  AF( 6 )
            AG0    =  AG( 6 )
            AH0    =  AH( 6 )
            AI0    =  AI( 6 )
C
            IF  ( IPINT .NE. 0 )   THEN
C
                IP   = 1
C
            ENDIF
C
            IF  ( IP .EQ. 1 )    THEN
C
                GO  TO  200
C
            ENDIF
C
      ENDIF
C
      PERSAT  = 1.0E+02 * AQ2 / ( AS1 * AL6 * 6490.)
C
      P       =  1.15E+06 * DROD * ( W1 - W1I ) / (2. * DT)
      BWTER   =  ( AQ2 / ( 6490. * AL6 ) ) - 0.0012
C
      IF  ( BWTER .LT. 0.0 )  THEN
C
            BWTER   =  0.0
C
      ENDIF
C
```

```
C AWTER = WEIGHT FRACTION OXYGEN IN THE ALPHA ZIRCALOY.
C AWTER TYPICALLY = 0.047.
C
C CONVERSION TO SI UNITS
C
      RETURN
C
C
 3100 CONTINUE
C
      RETURN
C
C
 2771 FORMAT("****** DECREASE IN BETA LAYER IS GREATER",/,
     *" THAN 1/E INITIAL LAYER...TIME STEP TOO LARGE OR BETA LAYER",/,
     ** TOO DEPLETED.")
C
C
 5020  FORMAT(//20X,'DIFFUSION IS OCCURRING TOO RAPIDLY FOR CEBILD
     * TO ACCURATELY CALCULATE OXYGEN CONCENTRATIONS ' )
C
C
  901 FORMAT  ( //T2 , '****** INPUT ERROR DETECTED FOR FIRST TIME' )
C
C
  902 FORMAT  ( /T3 , 'DT =' , E12.5 , 2X , 'AM5 =' , E11.5 , 2X ,
     +          'DROD =' , E11.5 , 2X , 'YM =' , E12.5 / 2X , 'YS =' ,
     +          E12.5 , 2X , 'YSA =' , E11.5 , 2X , 'YSB =' , E11.5 ,
     +          2X , 'W1 =' , E11.5 )
C
C
  903 FORMAT  ( /T3 , 'AAO =' , E11.5 , 2X , 'ABO =' , E11.5 , 2X ,
     +          'ACO =' , E11.5 , 2X , 'ADO =' , E11.5 , 2X , 'AEO =' ,
     +          E11.5 / 2X , 'AFO =' , E11.5 , 2X , 'AGO =' , E11.5 ,
     +          2X , 'AHO =' , E11.5 , 2X , 'AIO =' , E11.5 )
C
C
  904 FORMAT  ( /T3 , 'AAI =' , E11.5 , 2X , 'ABI =' , E11.5 , 2X ,
     +          'ACI =' , E11.5 , 2X , 'ADI =' , E11.5 , 2X , 'AFI =' ,
     +          E11.5 / 2X , 'AFI =' , E11.5 , 2X , 'AGI =' , E11.5 ,
     +          2X , 'AHI =' , E11.5 , 2X , 'AII =' , E11.5 )
C
C
C
      END
      FUNCTION COXWTK(CTEMP)
C         ****** FUNCTION COXTHK RETURNS THE PARABOLIC OX-          ******
C         ****** IDATION CONSTANT FOR ZIRCALOY OXIDATION.           ******
C         ****** FOR TEMPERATURES OF 1273K-1853K DATA AND           ******
C         ****** ANALYSES FROM J.V. CATHCART OF ORNL ARE USED.      ******
C         ****** FOR TEMPERATURES IN THE RANGE OF 1853K-2100K,      ******
C         ****** DATA AND ANALYSES FROM V.F. URBANIC AND T.M.       ******
C         ****** HEIDRICK,"HIGH TEMPERATURE OXIDATION OF            ******
C         ****** ZIRCALOY-2 AND ZIRCALOY-4 IN STEAM", JOURNAL       ******
C         ****** OF NUCLEAR MATERIALS 75,(1978) ARE USED.           ******
C
C     COXWTK = OUTPUT PARABOLIC OXIDATION CONSTANT (KG**2/M**4*S)
C     CTEMP  = INPUT CLADDING TEMPERATURE (K)
C
      IF(CTEMP.GT.1853.) THEN
          COXWTK=10.852*EXP(-16610/CTEMP)
                ELSE
          COXWTK=2.0*16.8*EXP(-39670.0/(1.987*CTEMP))
                ENDIF
      RETURN
      END
      FUNCTION COXTHK(CTEMP,KPICK)
C
```

```
C       ****** FUNCTION COXTHK RETURNS THE GROWTH RATE              ******
C       ****** CONSTANT FOR OXIDE THICKNESS, OXYGEN-STABILIZED      ******
C       ****** ALPHA LAYER THICKNESS (INNER AND OUTER),AND          ******
C       ****** THICKNESS OF THE OXYGEN-STABILIZED ALPHA             ******
C       ****** LAYER BETWEEN THE OUTER AND INNER ALPHA              ******
C       ****** LAYERS. FOR TEMPERATURES OF 1273K-1853K              ******
C       ****** DATA AND ANALYSES FROM J.V. CATHCART ET              ******
C       ****** URAL ARE USED TO COMPUTE THE ZRO2 AND                ******
C       ****** OXYGEN-STABILIZED ALPHA THICKNESSES ON THE           ******
C       ****** OUTER SURFACE AND SIMILAR EQUATIONS FROM             ******
C       ****** P. HOFMANN OF THE KERNFORSCHUNGSZENTRUM              ******
C       ****** KARLSRUHE (KFK) FOR OXYGEN-STABILIZED ALPHA          ******
C       ****** LAYERS ON THE CLADDING INNER SURFACE WHEN            ******
C       ****** THERE IS PELLET-CLADDING MECHANICAL INTER-           ******
C       ****** ACTION (PCMI). FOR TEMPERATURES OF 1853K-            ******
C       ****** 2100K,DATA AND ANALYSES FROM V.F URBANIC AND         ******
C       ****** T.H. HEILEKER , "HIGH TEMPERATURE OXIDATION          ******
C       ****** OF ZIRCALLOY-2 AND ZIRCALOY-4 IN STEAM," JOURNAL     ******
C       ****** OF NUCLEAR MATERIALS 75,(1978) PP. 251-261, ARE      ******
C       ****** USED TO COMPUTE ZRO2 LAYER THICKNESS.                ******
C
C     COXTHK= OUTPUT GROWTH RATE CONSTANT (M**2/S)
C     CTEMP = INPUT CLADDING TEMPERATURE (K)
C     KPICK = INPUT INTEGER 1-4, WHERE:
C                 KPICK=1 IS GROWTH RATE CONSTANT FOR OXIDE THICKNESS.
C                 KPICK=2 IS GROWTH RATE CONSTANT FOR OXYGEN-STABILIZE
C                         ALPHA LAYER NEAREST OUTER CLADDING SURFACE.
C                 KPICK=3 IS GROWTH RATE CONSTANT FOR OXYGEN-STABILIZE
C                         ALPHA LAYER NEAREST UO2 FUEL.
C                 KPICK=4 IS GROWTH RATE CONSTANT FOR OXYGEN-STABILIZE
C                         ALPHA LAYER BETWEEN OUTER AND INNER ALPHA
C                         LAYERS.
C
C *** KPICK=1 ****************
      IF(KPICK.EQ.1.) THEN
C
        IF(CTEMP.GT.1853) THEN
C
      COXTHK=2.07E-06*EXP(-16014/CTEMP)
C
        ELSE
C
           COXTHK=2.0*(1.12569E-06)*EXP(-3.5690EE04/(1.987*CTEMP))
C
        ENDIF
C
      ENDIF
C
C *** KPICK=2 ****************
C
      IF(KPICK.EQ.2) THEN
C
           COXTHK=2.00*0.761490E-04*EXP(-4.81418E04/(1.987*CTEMP))
C
      ENDIF
C
C *** KPICK=3 ****************
C
      IF(KPICK.EQ.3) THEN
C
           COXTHK=0.32E-04*EXP(-4.9E04/(1.987*CTEMP))
C
      ENDIF
C
C *** KPICK=4 ****************
C
      IF(KPICK.EQ.4) THEN
C
           COXTHK=0.70E-04*EXP(-4.4E04/(1.987*CTEMP))
C
      ENDIF
C
      RETURN
      END
```

```
CCCCCCCCCCCCCCCCCCCCCCCCCCCCCCCCCCCCCCCCCCCCCCCCCCCCCCCCCCCCCCCCCCCCCCCCCCCCCCC
      PROGRAM LIZARD(INPUT,OUTPUT,TAPE5=INPUT,TAPE6=OUTPUT,TAPE1)
CCCCCCCCCCCCCCCCCCCCCCCCCCCCCCCCCCCCCCCCCCCCCCCCCCCCCCCCCCCCCCCCCCCCCCCCCCCCCCC
C
C     MODIFICATION OF THIS PROGRAM BY R. E. MASON WAS COMPLETED
C     JANUARY 1982.
C
      DIMENSION TI(900), TM(900)
      DIMENSION TII(900), TMI(900)
      DIMENSION TITLE(8)
C     TI= TIME(S)
C     TM = TEMPERATURE(K)
C     ADI = INITIAL OXYGEN CONCENTRATION (AT:)
C     YOXF = INPUT ZRO2 THICKNESS (MICRONS)
C     YALF = INPUT ALPHA LAYER THICKNESS (MICRONS)
C     XI = INPUT XI LAYER THICKNESS(MICRONS)
C     YO = INITIAL ZRO2 THICKNESS (MICRONS)
C     YS = INITIAL ZR(O) THICKNESS(MICRONS)
C     DROD =INITIAL ROD DIAMETER(MM)
C     AMSI =INITIAL CLADDING WALL THICKNESS(MM)
C     NT = NUMBER OF TIME-TEMPERATURE POINTS
C     NOXY = SWITCH TO BASE CALCULATIONS ON OXIDE THICKNESS
C     NALPHA=SWITCH TO BASE CALCULATIONS ON ALPHA LAYER THICKNESS.
C     NXI  = SWITCH TO BASE CALCULATIONS ON XI LAYER THICKNESS.
C     NPIF = SWITCH FOR INNER OXIDE CALCULATION
C     SWITCH VALUES ARE 0=NO AND 1=YES
C
      READ(5,99)(TITLE(I),I=1,8)
   99 FORMAT(8A10)
      WRITE(6,665)(TITLE(I),I=1,8)
  665 FORMAT(1H1,130("*")    ,//,5X,"COBILD PROFILE CALCULATIONS FOR",5X,
     +8A10,/,130("*"),////)
      JPETS = 0
      NI = 1
      READ(5,100) AMSI,DRODI,YBI,Y9I,YOXF,YALF,XI
      READ(5,101) NOXY,NALPHA,NXI,NPIF
      WRITE(6,202) AMSI,DRODI,YBI,Y9I,YOXF,YALF,XI,NOXY,NALPHA,NXI,NPIF
  101 FORMAT(4I5)
  202 FORMAT(T25,"INITIAL INPUT PARAMETERS",///,
     +25X,"INITIAL CLADDING WALL THICKNESS     =",1PE10.4,"(MM)      ",//,
     +25X,"INITIAL ROD DIAMETER                =",1PE10.4,"(MM)      ",//,
     +25X,"INITIAL ZRO2  THICKNESS             =",1PE10.4,"(MICRONS)",//,
     +25X,"INITIAL ZR(O) THICKNESS             =",1PE10.4,"(MICRONS)",//,
     +25X,"POSTTEST ZRO2 THICKNESS             =",1PE10.4,"(MICRONS)",//,
     +25X,"POSTTEST ZR(O) THICKNESS            =",1PE10.4,"(MICRONS)",//,
     +25X,"POSTTEST XI THICKNESS               =",1PE10.4,"(MICRONS)",//,
     +25X,"COMPARISON USING ZRO2 LAYER  1 = YES:  0 = NO ",I5,//,
     +25X,"COMPARISON USING ZR(O)LAYER  1 = YES:  0 = NO ",I5,//,
     +25X,"COMPARISON USING XI   LAYER  1 = YES:  0 = NO ",I5,//,
     +25X,"CALCULATION TO INCLUDE INNER LAYER 1=YES: 0=NO ",I5,////)
C
C
      YB = YBI * 1.0E-6
      YS = Y9I * 1.0E-6
      AMS = AMSI * 1.0E-3
      DROD = DRODI * 1.0E-3
      READ(5,200) NT,NPETS, DTI, F, FAX, FSTEP
      WRITE(6,200) NT,NPETS, DTI, F, FAX,FSTEP
  200 FORMAT(2I5, 4E10.2)
C     DTI IS THE MAXIMUM TIME STEP ALLOWED (S).
C     NPETS IS THE PRINTOUT TIME INTERVAL.
C     FAX IS THE FINAL MULTIPLICATION FACTOR.
C     F IS THE INITIAL MULTIPLICATION FACTOR.
C     FSTEP IS THE MAXIMUM TIME STEP ALLOWED.  LARGER TIME STEPS WILL
C     BE BROKEN INTO N TIME STEPS OF SIZE FSTEP(S).
C
      READ(5,300)(TII(I),TMI(I),I=1,NT)
      WRITE(6,301)
  301 FORMAT(" INPUT",9X,"TIME(S)",9X,"TEMPERATURE",7X,"INTERFACE PRESSU
```

```
      READ)
      WRITE(6,300)(TII(I),TMA(I),I=1,NT)
  100 FORMAT(7F10.4)
  300 FORMAT(2F20.4)
C
C
C       CALCULATIONS BEGIN FROM TAMB TII(1)
C
    6 CONTINUE
      YGT=YP
    9 CONTINUE
      YG=YGT
      TAMBW = TII(1)
      YLA=YG
      AAO=0.0012
      ABO=0.0012
      ACO=0.0012
      ADO=0.0012
      AEO=0.0012
      AFO=0.0012
      AGO=0.0012
      AHO=0.0012
      AIO=0.0012
      AAI=0.0012
      ABI=0.0012
      ACI=0.0012
      ADI=0.0012
      AEI=0.0012
      AFI=0.0012
      AGI=0.0012
      AHI=0.0012
      AII=0.0012
      YYA=0.0
      YYB=0.0
      WI=0.0
       F  = 0.0
       PERSAT = 0.0
       QWTFR  = 0.0
       ALG  = 0.0
      IP=0.0
      KKAP  = 0
      IP2=0.0
       T1  = 600.0
       T2  = 600.0
       PIF  = NPIF
       PANI  = PIF
    1 CONTINUE
      S1=YG1
      S2=YGI
      S3=YGA
      S4=YGB
      S5=AAO
      S6=ABO
      S7=ACO
      S8=ADO
      S9=AEO
      S10=AFO
      S11=AGO
      S12=AHO
      S13=AIO
      S14=AAI
      S15=ABI
      S16=ACI
      S17=ADI
      S18=AEI
      S19=AFI
      S20=AGI
      S21=AHI
      S22=AII
      S23=WI
```

```
      S24=P
      S25=PERSAT
      S26=BWTFR
      S27=ALB
    5 CONTINUE
      Y8=S1
      Y9=S2
      Y9A=S3
      Y9B=S4
      AAO=S5
      ABL=S6
      ACO=S7
      ADO=S8
      AEO=S9
      AFO=S10
      AGO=S11
      AHO=S12
      AIO=S13
      AAI=S14
      ABI=S15
      ACI=S16
      ADI=S17
      AEI=S18
      AFI=S19
      AGI=S20
      AHI=S21
      AII=S22
      WI=S23
      P=S24
      PERSAT=S25
      BWTFR=S26
      ALB=S27
      J = 1
   10 CONTINUE
      TI(J) = TII(J)
      PIF = PIF
      TM(J) = TMI(J)*F
      IF(J .GT. NT) GO TO 12
      IF(J-1 .LE. 0) THEN
      TIL = TII(1) - 0.0001
      ELSE
      TIL = TII(J-1)
      ENDIF
      DT = TII(J) - TIL
   11 CONTINUE
      IF(DT .LE. DTI) GO TO 13
      T1 = T2
      T2 = (T2 + (TMI(J) * F - T2) * TIMNOW/TI(J))
      DT = DTI
      GO TO 14
   13 CONTINUE
      T1 = T2
      T2 = TMI(J)*F
   14 CONTINUE
      IP=0
      IP2=0
      PINT = 0.0
      IF (PINT.EQ.0.0) GO TO 6
      IP=1
      IP2=2
    6 CONTINUE
      CALL COBILD ( T1, T2, DT,AMB, DRGD, PINT, IP2, Y8, Y9,
     *                    Y9A,Y9B,AAO,ABO,ACO,ADO,AEO,AFO,AGO,AHO,AIO,
     *                    AAI,ABI,ACI,ADI,AEI,AFI,AGI,AHI,AII, WI, P,
     *                    PERSAT , BWTFR ,ALB,KRAP)
C
      TIMNOW = TIMNOW + DT
      Y8C = Y8 * 1.0E+6
      Y9C = Y9 * 1.0E+6
      Y9AC = Y9A * 1.0E+6
```

```
      ALBC = ALB * 1.0E+3
      YBBC = YBB * 1.0E+6
      YAAC = YBC + YBC
      TPETS = NI * DPETS
      TPETS2 = TPETS + DTI

      IF(TIMNOW .GE. TPETS2) DPETS = 0
      IF(TIMNOW .GE. TPETS .AND. TIMNOW .LT. TPETS2)THEN

      NI = NI + 1
      WRITE(6,3)
      DPETS = 1


      WRITE(6,3)
      WRITE(6,2) J,T1,T2,F,DT,     TMI(J),TIMNOW,TI(J),TII(J),TM(J),AMS
    3 FORMAT(5X,"J,T1,T2,F,DT,TMI(J),TIMNOW,TI(J),TII(J),TM(J),AMS")
      WRITE(6,222) YBC,YBC,YYAC,YYBC,ALBC,W1,PERSAT,BWTFR,TIMNOW,F,
     +AAD,ABD,ACD,ADD,AED,AFD,AGD,AHD,AID
      WRITE(6,112)
      ENDIF
      WRITE(6,2) J,T1,T2,F,DT,     TMI(J),TIMNOW,TI(J),TII(J),TM(J),AMS

      WRITE(6,222) YB,YS,YYA,YYB,YAIC,YCAF,YALF,XI,ALB,W1,PERSAT,
     +BWTFR,TIMNOW,F,AAD,ABD,ACD,ADD,AED,AFD,AGD,AHD,AID
      WRITE(6,112)
      DT = TII(J) - TIMNOW
      IF(TIMNOW .GE.TII(NT))GO TO 12
      IF(TIMNOW .LT. TI(J)) GO TO 11
      J = J + 1
      GO TO 10
   12 CONTINUE
      IF(F .GT. FAX) GO TO 50
      WRITE(6,113)
      WRITE(6,222) YBC,YBC,YBAC,YYBC,YAIC,YCAF,YALF,XI,ALBC,W1,PERSAT,
     +BWTFR,TIMNOW,F,AAD,ABD,ACD,ADD,AED,AFD,AGD,AHD,AID
      IF(NPIF .GT. 0.0) THEN
      WRITE(6,223) AAI, ABI, ACI, ADI, AEI, AFI, AGI, AHI, AII
      ENDIF
      WRITE(6,301)
  444 FORMAT(//,T45,"TIME, TEMPERATURE, INTERFACE PRESSURE",
     +/,T45,35("*")    ,//)
      DO 60 I=1,NT
      TX = TII(I)
      TY = TMI(I) * F
      WRITE(6,300) TX, TY
   60 CONTINUE
  223 FORMAT(9E9.3)
      WRITE(6,113)
      IF(NOXY .GE. 1 .AND. YCAF .LE. YBC) GO TO 50
      IF(NALPHA .GE. 1 .AND. YALF .LE. YBC) GO TO 50
      YXI = YCXF + YALF
      YX = YBC + YBC
      IF(NXI .GE. 1 .AND. YX .GE. XI) GO TO 50

C     THIS ENDS THIS CALCULATION SET AND REINITIALIZATION BEGINS AFTER
C     THIS CARD.


      F = F + FSTEP
   21 FORMAT(6E20.4)
      TIMNOW = TII(1)
  113 FORMAT(//,132("*"),/,132("*"),//)
      GO TO 5
   50 WRITE(6,666)(TITLE(I),I=1,8)
      YYT=YBAC + YBBC
  666 FORMAT(1H1,130("*")    ,/,5X,"FINAL STATE FOR MATCHED LAYER ",5X,
     +8A10,/,130("*"),////)
      WRITE(6,334) YBC, YBC, YX, YYT , YCXF, YALF
  334 FORMAT(T45,"ZRO2 THICKNESS AT END OF TRANSIENT(MICRON=",1PE10.4,//,
```

```
     +///,T45,"ZR(J) THICKNESS AT END OF TRANSIENT (MICRON)=",1PE10.4,///,
     +T45,"XI    THICKNESS AT END OF TRANSIENT (MICRON)=     ",1PE10.4,///,
     +T45,"INNER ZR(O) THICKNESS AT END OF TRANS (MICRONS)= ",1PE10.4,//,
     +T45,"ZR OXIDE THICKNESS - METALLOGRAPHIC (MICRONS)=   ",1PE10.4,//,
     +T45,"ZR(O) THICKNESS - METALLOGRAPHIC (MICRONS)=      ",1PE10.4,////)
112   FORMAT(132(1H*))
222  FORMAT(T25,"ZR-OXIDE THICKNESS                    =",1PE10.4,"(MICRONS)",//
     +25X,"ZR(O) THICKNESS NEAR CLADDING SURFACE=",1PE10.4,"(MICRONS)",//
     +25X,"ZR(O) THICKNESS NEAR FUEL            =",1PE10.4,"(MICRONS)",//
     +25X,"ZR(O) THICKNESS-MIDDLE               =",1PE10.4,"(MICRONS)",//
     +25X,"XI LAYER THICKNESS                   =",1PE10.4,"(MICRONS)",//
     +25X,"INPUT ZRO2 THICKNESS                 =",1PE10.4,"(MICRONS)",//
     +25X,"INPUT ALPHA LAYER THICKNESS          =",1PE10.4,"(MICRONS)",//
     +25X,"INPUT XI LAYER THICKNESS             =",1PE10.4,"(MICRONS)",//
     +25X,"BETA ZR THICKNESS                    =",1PE10.4,"(MM)      ",//
     +25X,"OXYGEN UPTAKE THROUGH OUTER SURFACE  =",1PE10.4,"(M)",///,
     +25X,"PERCENT SATURATION OF BETA           =",1PE10.4,///,
     +25X,"AVERAGE OXYGEN CONCENTRATION IN BETA =",1PE10.4,"(WT.FR.)",//,
     +25X,"TIME                                 =",1PE10.4,"(S)",//
     +25X,"TEMPERATURE MULTIPLICATION FACTOR    =",1PE10.4,//
     +,5X,"OXYGEN CONCENTRATIONS IN BETA(WT.FR.)",9(1PE9.3,1X),//)
 55  CONTINUE
 56  CONTINUE
  2   FORMAT(I5,12E10.4)
      STOP
      END
```

EG&G Idaho, Inc.
P.O. Box 1625
Idaho Falls, Idaho 83415